View metadata, citation and similar papers at core.ac.uk

brought to you by CORE

provided by University of New Mexico

University of New Mexico
UNM Digital Repository

Mechanical Engineering ETDs | Engineering ETDs

7-12-2014

Exploring the Performance of Active Thermal Tiles for Space Applications

Rachel K. Delaney

Follow this and additional works at: https://digitalrepository.unm.edu/me_etds

Recommended Citation
Delaney, Rachel K.. "Exploring the Performance of Active Thermal Tiles for Space Applications." (2014).
https://digitalrepository.unm.edu/me_etds/80

This Thesis is brought to you for free and open access by the Engineering ETDs at UNM Digital Repository. It has been accepted for inclusion in Mechanical Engineering ETDs by an authorized administrator of UNM Digital Repository. For more information, please contact disc@unm.edu.

Rachel K. Delaney
Candidate

Mechanical Engineering
Department

This thesis is approved, and it is acceptable in quality and form for publication:

Approved by the Thesis Committee:

C. Randall Truman, Chairperson

Arsalan Razani

Andrew Williams

Derek Hengeveld

EXPLORING THE PERFORMANCE OF ACTIVE THERMAL TILES FOR SPACE APPLICATIONS

by

RACHEL K. DELANEY

BACHELOR OF SCIENCE, MECHANICAL ENGINEERING
UNIVERSITY OF NEW MEXICO, 2011

THESIS

Submitted in Partial Fulfillment of the
Requirements for the Degree of

Masters of Science
Mechanical Engineering

The University of New Mexico
Albuquerque, New Mexico

May, 2014

ACKNOWLEDGEMENTS

I would like to thank all of my friends and family for encouraging me as I pursued this degree. I could not have done it on sheer stubbornness alone. I would also like to thank Dr. Truman for his inputs and his willingness to shape me and guide me along the way. I also wish to express my gratitude to my colleagues at the Air Force Research Laboratory – Space Vehicles Directorate: Derek Hengeveld, Andrew Williams, Hans-Peter Dumm, Brent Taft, Joy Stein, Nick Boucher, Julio Alvarado, Steven Lockyer, Kailey Brunetto, Sally Smith and many other of my coworkers for helping me in immeasurable ways whether it was pointing me in the direction for analyzing my data, collaborating to determine the proper test procedure, proofreading my documents or even simply helping me assemble and disassemble. I could not have done any of this without them.

The software and control simulation were developed by Infoscitex under a Small Business Innovation Research initiative. This work was supported by the Air Force Research Laboratory – Space Vehicles Directorate.

EXPLORING THE PERFORMANCE OF ACTIVE THERMAL TILES FOR SPACE APPLICATIONS

by

Rachel K. Delaney

B.S., Mechanical Engineering, University of New Mexico, 2011

M.S., Mechanical Engineering, University of New Mexico, 2014

ABSTRACT

The Active Thermal Tiles (ATTs) experiment explores another option for managing electronic component temperatures onboard spacecraft. The ATTs are based on thermoelectric devices that can alter the thermal gradient between the bus and component. Because ATTs do not rely on fluids or moving parts, they are highly reliable devices which make them attractive for use in spacecraft. An ATT experimental ground unit was tested in a vacuum chamber under 88 different conditions over a temperature range of 280K to 310K. The power supplied to the electronic component was varied between 5W and 40W, and the current running through the ATTs was varied between 0.0A and 3.0A. Conductance and the coefficient of performance were measured, and a performance map was created. In addition, the power used by the ATTs was compared against the power used by survival heaters. Results showed the ATTs require less power to create the same temperature differential as survival heaters proving ATTs are more efficient than a traditional survival heat approach. Also, a computer simulation of the ATT was calibrated and used to compare the two control methods for the ATTs: PID or On-Off. PID control was up to two times as efficient as On-Off control. Ground tests were run to confirm the results from the simulation.

TABLE OF CONTENTS

List of Figures

List of Tables

Nomenclature

COP_C	Cooling coefficient of performance
COP_H	Heating coefficient of performance
$\dot{Q}_E$	Heat flow from the electronics box into the radiator
$\dot{Q}_{E,\infty}$	Heat flow from the electronics box into the surroundings
T	Temperature
ΔT	Change in temperature between TED hot side and the cold side
$\dot{W}_{ATT}$	ATT power
$\dot{W}_{BusA}$	Bus A power
$\dot{W}_E$	Electronics box power
$\dot{W}_{E_{ATT}}$	Electronics box power during ATTs only heating cases
$\dot{W}_{E_{Htrs}}$	Electronics box power during heaters only heating cases
$\dot{W}_{Htrs}$	Electronics box heater power

1. Introduction

1.1. Thermal Control Systems for Spacecraft

Space is an environment that offers a wealth of opportunities for research and application. Technologies developed because of satellites and human spaceflight have assisted in saving lives and making life on earth more convenient. Satellites aid in predicting weather and studying the climate. Such forecasts can determine crop yield as well as prevent deaths and extreme damage when an area is faced with a particularly dangerous storm or other natural disaster. Communication is now possible in remote areas where it was not available before. One can determine location and receive directions to a new destination via the satellite-based Global Positioning System (GPS). Other fields have technologically benefited from space exploration as well, such as the medical field and electronics industry. Materials that had to be developed and tested to travel through the vacuum of space needed to be lightweight, durable, and strong. Such materials were then used in the medical field for implants, surgical tools, or other means of repairing injuries or saving lives (space-exploration.org, 2013).

Not only does space flight benefit the world's technological capabilities, but also its global economics. Space exploration creates high-paying jobs not only for those working in the space program, but also in areas supporting it (Coalition for Space Exploration, 2010). Satellites can also be used to discover valuable natural resources in lands thought to be worthless and desolate, causing economies to boom. Some discredit space exploration, claiming the benefits are few, but space exploration and its products and technological advances have affected our daily lives in ways one could not imagine and clearly for the better. However, accessing such prospects is challenging.

Several environmental factors must be considered when designing a spacecraft. First, micrometeoroids and spacecraft debris can cause significant damage due to the high speeds involved in space flight. The vacuum of space must also be considered. Seemingly insignificant things such as air pockets inside the structure of the spacecraft can cause substantial problems when a satellite is introduced into the space environment. Another problem is outgassing which occurs when gas, previously trapped or dissolved in a material, is released when the material is placed inside a vacuum. These gases can condense and interfere with critical components such as spacecraft optics. Finally, the thermal environment of space is a factor that cannot be overlooked. The extreme temperatures between sunlight and shadow are 250°F and -250°F (National Aeronautics and Space Administration, 2012). In addition, there are different forms of radiation that need to be taken into account when designing a spacecraft. Albedo, infrared (IR), and solar radiation must be considered.

Thermal control systems are designed and developed to overcome the challenges of the harsh thermal environment of space while managing electronic components within a spacecraft. Designing thermal control systems for spacecraft can be an in-depth process and costly to implement. First of all, each component of the satellite must be evaluated to determine thermal control requirements and evaluate methods to meet them. Then there is a validation phase, where a design is created based on the budget of the project and the schedule for which it needs to be completed. Then the final design is developed and installed on the spacecraft (Gilmore, 2002). Most satellites are fitted with custom thermal control systems near the end of production to assure proper performance and an acceptable fit.

There are several different forms of thermal control used on satellites today. One example is multi-layer insulation (MLI). MLI is a passive form of insulation featuring several different layers of metal-coated Kapton sandwiching lightweight netting. The layers each reflect a certain amount of radiation back towards the source, resulting in very little heat loss (Gilmore, 2002). Also, satellites can feature louvers, which function like shutters. They can be opened when electronics are too hot and closed when electronics need to be warmed. Another form of thermal protection can be fluid loops or heat pipes. These are piping networks filled with coolant such as Freon, ammonia, or water – all of which draw heat away from warm components.

Many areas of everyday life are affected by a satellite's ability to perform as expected whether it is used for communications, GPS, or weather forecasting. In order to function properly, a satellite must be designed with means for adequate temperature control. Spacecraft thermal control is a field that is always open for improvement and new alternatives. The focus of this research is a promising alternative called the Active Thermal Tile (ATT), a type of thermoelectric device (TED).

1.2. Thermoelectric Devices

There are several different ways to implement thermal control on components on a satellite, but it has been suggested that ATTs may serve as yet another suitable option for temperature control on a satellite. Developed by Infoscitex as a Small Business Research Innovation project with the Air Force Research Laboratory, ATTs utilize thermoelectric devices (TEDs) and can be implemented and adjusted to fit a wide range of low heat transfer electronic components.

Many advantages can be found when using TEDs to cool and heat. First, they are solid-state devices that have no moving parts, thus reducing noise and vibration and increasing reliability. They also do not require fluid to aid in their energy conversion process, which makes them light weight. Another advantage is their small size. All of these aspects make them optimal choices when it comes to situations where heat transfer needs to be controlled (Riffat and Ma, 2003) and make them prime candidates for space applications where reliability, mass, size, and utility in microgravity are driving design considerations.

While TEDs have many useful attributes, they tend have a low coefficient of performance (COP) and limited heat transfer capacity. This means that their applications are limited to cooling or heating electronics characterized by only low heat transfer (Simons and Chu, 2000). Despite this, TEDs have been used on several spacecraft. Examples range from pollution monitoring satellites to the Hubble Space Telescope (Peabody et al., 2007; Copeland and Oren, 1975). However, while the devices have been used in orbit, very little research has been published comparing their on-ground performance with their on-orbit performance.

1.3. Literature Review and Experimental Objectives

1.3.1. Review of Related Literature

TEDs operate using the Peltier effect which "occurs if a current is circulated around a loop of two dissimilar materials; heat is absorbed at one junction and released at the other" (Mole et al., 1972). These devices use electrical energy to transfer heat to or from an object, thereby heating or cooling it. In order for the TED to cool, a current is passed through pairs of two different types of semiconductor materials that have formed a

junction, shown in Figure 1. One material contains positive charges and is referred to as p-type material, while the other contains negative charges and is known as n-type material (DiSalvo, 1999). As the electrons pass from the n-type material and into the p-type material, heat is absorbed from the environment. Consequently, if the current is reversed, heat is released into the environment.

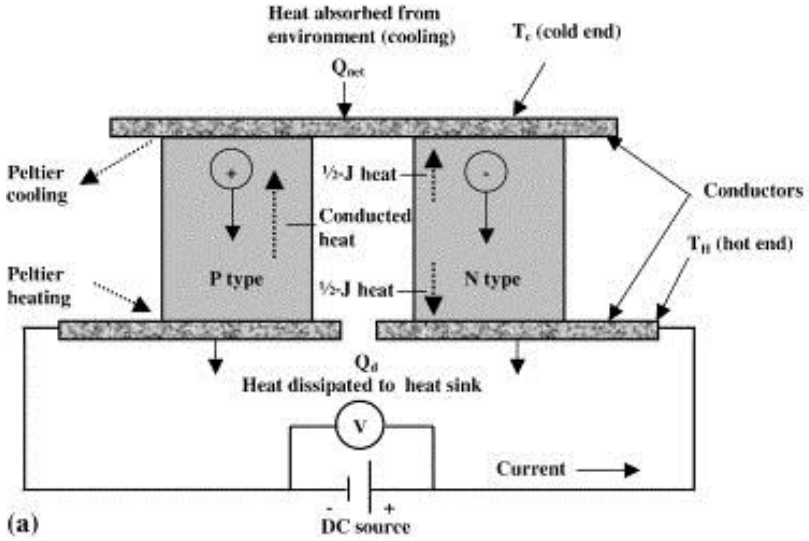

Figure 1: Thermoelectric device cooling schematic (Mole, et al., 1972).

The study of thermoelectricity was first developed in 1834 after the discovery of the Peltier effect, yet there were not any major applications until the mid-1950s. A.V. Ioffe developed the idea of using compounds composed of elements from the lower part of the periodic table. His ideas led to the use of materials such as bismuth, lead telluride, and bismuth telluride for thermoelectric applications (Nolas, et al., 1998).

Since then, TED research has focused on improving heating/cooling efficiency and expanding their applications. The COP for TEDs is not as high as it is with other forms of cooling. Typically, a single stage TED has a COP between 0.4 and 0.7. However, that number can increase with optimized, custom TEDs or as more stages are

added to the TED (Marlow Industries, 2012). Adding more stages will increase the device's size and weight, so research has been conducted to make COP improvements without compromising the size and weight aspects that make TEDs desirable (Laird Technologies, 2010).

Chein and Huang (2000) ran a number of tests to see which temperatures resulted in the highest efficiencies for TEDs. Others have focused on optimizing a TED's COP by different means. For example, Wijingaards et al. (2000) writes about changing the semiconductor materials that make up the TED from the usual Bi_2Te_3 to polySi.

Research has been conducted concerning the applications of a TED. Simons and Chu (2000) mention that IBM has been researching TEDs since the 1960's. They researched using TEDs to cool components of electronic equipment, and also investigated how well a TED could cool chips on a wafer, shown in Figure 2. While they were able to achieve some cooling, they determined TED technology needed to advance for it to be applicable to their work. The attainable COP and the heat pumping capability of the TEDs used in the experiment were not good enough to affect the electronics in a way they deemed acceptable. However, they did admit the concept had potential benefits.

Walker et al. (2004) also analyzed the idea of using thermoelectric coolers to cool electronics. The model involved testing TEDs under several different conditions such as uniform heating and cooling, nonuniform heating and uniform cooling, and nonuniform heating and nonuniform cooling. Those cases also involved different heat loads, ranging from 10W to 60W. After the data was compiled, the results were compared with data from electronics with no cooling mechanism.

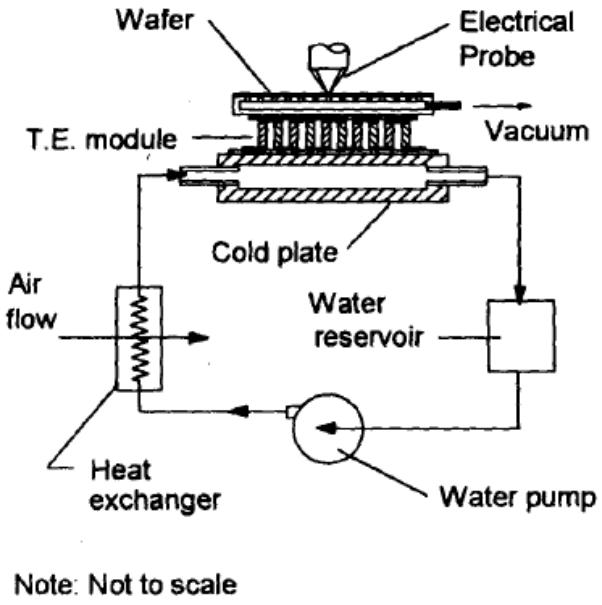

Figure 2: Simons and Chu TED experimental setup (Simons, 2000).

Walker's research found that a TED would provide better performance in realistic situations when heating is localized, such as on a chip compared to standard cooling devices. In fact, the more localized the heat was, the better the performance of the TED (Walker et al., 2004). However, different parameters were noted that would need to be evaluated in order to optimize performance. These include: size and shape of the TED array elements, how including power and sensor circuitry in each element would affect both the cost and the effectiveness of each element, and how each localized controller would use information gathered from each neighboring array element.

Cheng et al. (2005) tested the performance of a silicon-based thermoelectric device as it cooled a high-powered light emitting diode (LED). Two TEDs were tested – one with 12 pairs of "thermoelectric legs" and the other with 16 pairs. The experimental setup started out at room temperature, and the difference between the LED and room temperature was measured as the current was increased. They recorded a difference of

approximately 11.5°C between ambient temperature and the TED for the 12 pair device. The graphs of the results are shown in Figure 3. The 16 pair device resulted in a temperature difference of approximately 24.9°C. The resulting plots were parabolic because after a certain point, most of the input current begins transferring to joule heating and the TED is not as effective. After the results of the experiement were analyzed, it was determined that a silicon-based TED can be used as an active cooler because it successfully lowered the thermal resistivity of the LED.

Ramanathan and Chrysler (2006) analyzed the idea of using TEDs to cool electronic components in a microprocessor. TEDs were modeled as positioned on the backside of a die and directly over a hot spot that was assumed to have a heat flux of 800 W/cm^2. Using series of equations, the graph in Figure 4 was developed to show the differences in the temperature of the electronics both with the different thermoelectric devices, and without the thermoelectric devices. It was concluded that TEDs offer potential thermal benefits and determined that the integration of TED in a microprocessor is a "significant and revolutionary change".

Wang et al. (2007) modeled and experimentally measured the reduction in temperature caused by TEDs. In these experiments, a TED was connected to a silicon chip by means of a copper "mini contact pad" that was found to greatly improve the TED's cooling performance. Different sizes of mini contact pads were tested under different power levels.

Wang et al. (2007) concluded that this type of cooling had "great potential application for on-chip hot spot cooling…by concentrating the thermoelectric cooling on

small regions of the silicon chip". Figure 5 shows the temperature of the chip, and shows strong similarities to Ramanathan's research in Figure 4.

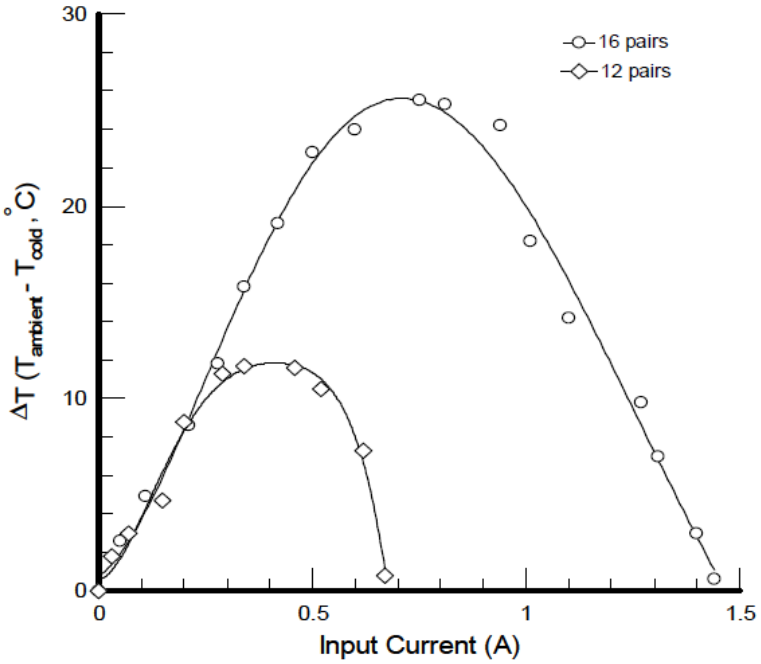

Figure 3: The performance of a silicon-based TED cooling a high-powered LED (Cheng et al., 2005).

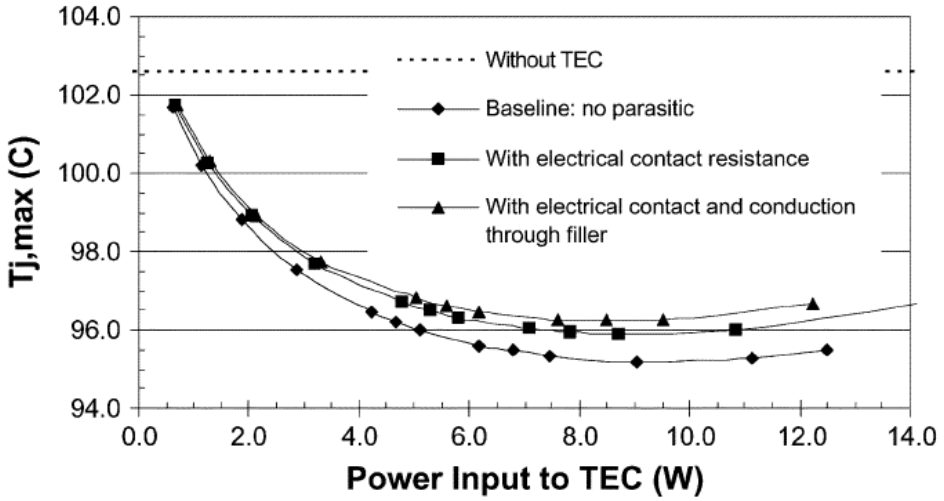

Figure 4: Ramanathan and Chrysler (2006) TED experiment results.

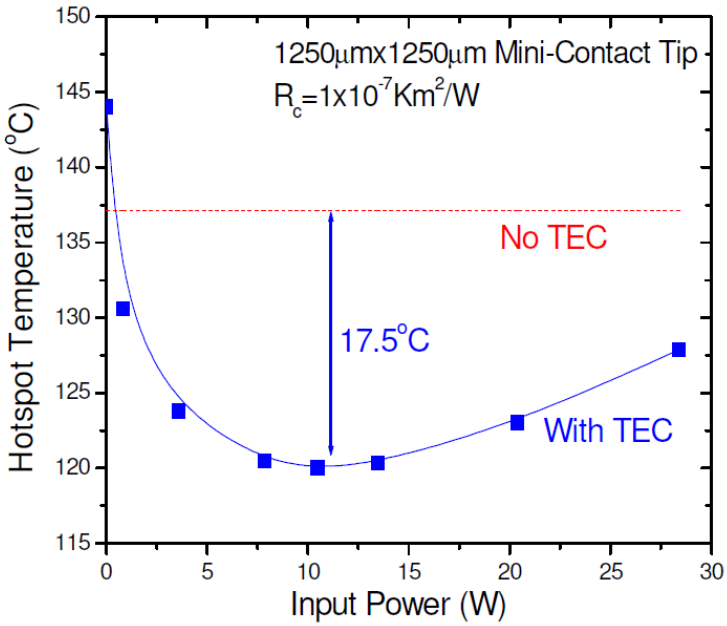

Figure 5: Hot spot temperature variation versus TED power (Wang et al., 2007).

Later, Alley et al. (2008) performed tests using embedded TEDs for thermal control on an Intel mobile Core 2 Duo processor. After installing the TEDs on the central processing unit (CPU) die, a maximum temperature difference of 10°C was achieved through passive and active cooling.

Tiezhu et al. (1999) ran experiments on a satellite using TEDs to cool the electronics on-orbit. The sole purpose of this experiment was to test if TEDs could be successful in keeping the temperature gradients on the satellite within a nominal range. The satellite was in orbit for 8 days and it was found the TEDs were able to keep the electronics within a desired temperature range while drawing a maximum current of 1.43A. However, there was no ground testing involves with these tests.

Peabody et al. (2007) implemented TEDs on the Wide Field Camera 3 on the Hubble Space Telescope. The instrument uses the devices to both cool the detectors on the camera and thermally isolate the detectors from the rest of the instrument. While they

were efficient in cooling, Peabody et al. state there was a slight difference between the vendor's power versus cooling performance curves and the actual results due to how the vendor predicted the curve. They found an improvement of 5% was needed. Thus, to compensate, they ran their electronics at 95%. Because of this difference, and similar situations with other components, Peabody et al. insisted that the thermal design of a spacecraft be ground tested, and all power associated with active control devices be predicted beforehand.

1.3.2. Summary and Objectives

Previous work with thermoelectric devices (TEDs) tested their ability to cool electronics in terrestrial environments. There have also been limited on-orbit tests of spacecraft mounted TEDs, but comparisons of ground and on-orbit performance have not been well documented. The objective of the present work was to develop a ground-based performance map and control study of the ATTs. The results of this effort will be delivered to and utilized by Air Force Research Laboratory (AFRL) personnel to support on-orbit testing on the International Space Station (ISS).

To accomplish this objective, the following tasks were proposed.

1. Examine the modes of operation that are available with the ATTs and determine how to measure them. Then develop a test procedure and prepare an adequate test setup that will explore the passive cooling and heating properties of the tiles, their ability to cool both with and against the thermal gradient, and their ability to heat both with and against the thermal gradient.

2. Install experimental components such as instrumentation, hardware, etc., and integrate support systems to be used to create an acceptable setup for simulating and monitoring a space environment and gathering applicable data.
3. Conduct 24-hour vacuum tests with varying temperature gradients to test all aspects of the ATT operating conditions (passive and active cooling and heating).
4. Use the data collected from the tests to develop a performance map, determining the coefficient of performance for each mode of operation (enhanced cooling, refrigeration, enhanced heating) and heat pump conditions for the various TED operating currents, radiator temperatures, and component heat loads. Results will be documented in order to be compared to on-orbit experiments on the International Space Station.
5. Use data collected from performance tests to calibrate a numerical model of the ATT test setup in order to simulate test conditions.
6. Find control variables for a proportional-integral-derivative (PID) controller and develop a control strategy needed for on-orbit testing of ATTs.

2. Experimental Method-Performance Testing

2.1. System Configurations

The Active Thermal Tiles (ATTs) are designed to be installed on spacecraft to actively regulate electronic component temperatures. To evaluate their performance under a wide-range of conditions, two similar test units (flight and flight spare) were designed, developed, and assembled by a team at the Air Force Research Lab (AFRL) prior to the work presented here. The flight unit was installed on the International Space Station, while the flight spare was used for ground testing at AFRL facilities. Both test units were designed and developed to simulate both a bus (heat sink) and electronic component (heat source). The ATTs were then sandwiched between source/sink and tested under a wide-range of conditions. Figure 6 illustrates how the components on a spacecraft would need to be arranged to be thermally managed.

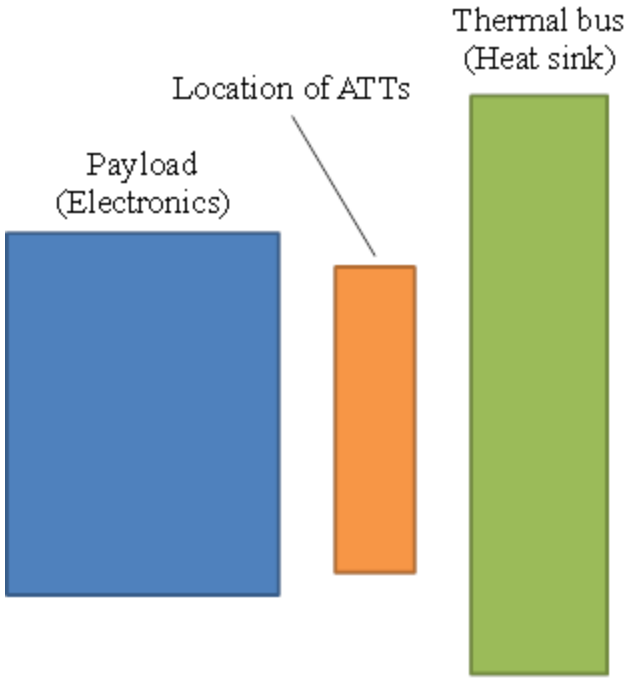

Figure 6: Thermal components on a spacecraft.

Six components make up the actual ATT experiment: an electronics box (heat source), an electronics box lid, a radiator (heat sink), two side support brackets, and an L bracket. The radiator dissipates waste heat, the L bracket allows the front of the radiator to be fastened to a baseplate if necessary (this feature is not used in this test setup), while the two side support brackets hold the radiator normal to the base. All of those components are made of 6061-T651 aluminum. The entire radiator structure is bolted to the two side supports by 35 ¼”-28 screws. When assembled, the dimensions of the assembly are 16” wide by 13.125” deep, by 24” tall. The structural setup is shown in Figure 7.

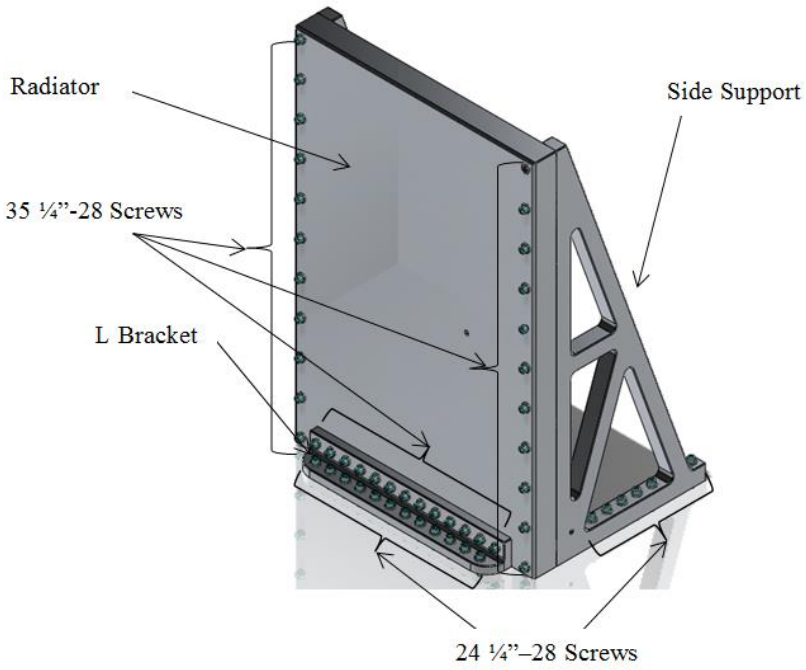

Figure 7: ATT experiment structure (shown without the cold plate or cold plate mount).

The radiator simulates the “bus” and was fitted with four resistance temperature detectors (RTDs) and two 20 W heaters. These heaters, along with two separate cold

plates, keep the radiator at a set temperature. There is also a sun sensor on the radiator to aid in data reduction efforts by sensing the sunlight status on the radiator.

An electronics box is mounted in the center of the back of the radiator to simulate an electronic component. This unit includes four 10W resistance heaters, printed circuit board (PCB) that controls the electronic components on the setup, and four RTDs. The electronics box lid is attached using four #6-32 screws. An aerogel blanket insulates the electronics box to help reduce heat loss to the surroundings.

The ATTs themselves, shown in Figure 8, are sandwiched between the radiator and the electronics box to affect the flow of heat between them. This is done using 8 #8-32 flathead screws that pass through clearance holes in the electronics box bottom and thread into helicoils in the back of the radiator. The ATT is not just a thermoelectric device (TED), but an assembly of components that offers another way of cooling and heating electronics. This assembly includes the TED, a bypass circuit that maintains ATT functionality if one module were to fail, and plug-and-play connections. This assembly as well as the ATT orientation can be seen in Figure 9.

To properly ground test the ATTs, they needed to be placed in an environment to simulate thermal conditions a spacecraft would experience on-orbit. The ATT setup was housed in a bell jar-style vacuum chamber 10^{-5} torr or less for all experiments. Electronics box heaters simulate the heat loads electronics generate during a mission. The radiator simulates the bus or thermal sink over a range of temperatures using patch heaters and two cold plates. The cold plates were plumbed, using feedthroughs and VCR fittings, to a cycling refrigerating bath filled with cooled Syltherm. The cold plate mounts' configuration is shown in Figure 10 and an example of their connection to the

refrigerating baths is shown in Figure 11. Figure 12 shows how the experimental setup simulates a spacecraft.

To insulate the assembly from any outside thermal interference, an MLI blanket with a black Kapton outer layer covered the entire set. The blanket was attached using Kapton tape. All interfaces are dry bolted with the exception of the interfaces between the ATT's TEDs and the radiator between the TEDs and the electronics box. These interfaces utilized an eGRAF thermal interface material to increase thermal conductivity.

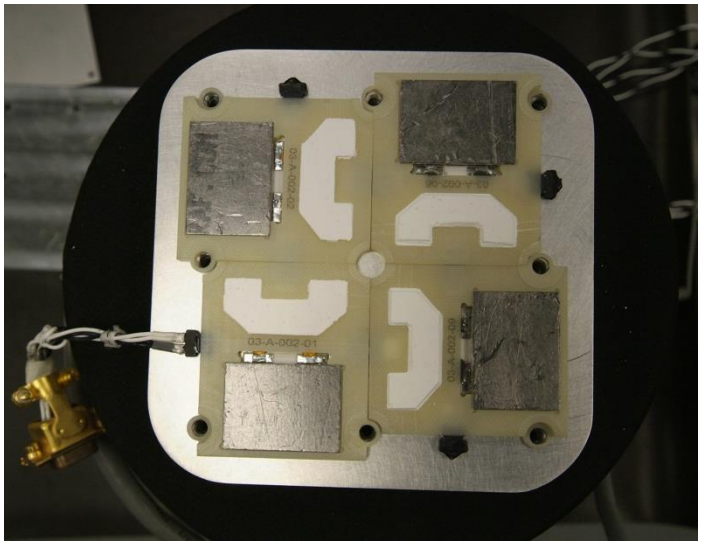

Figure 8: ATT assembly and orientation.

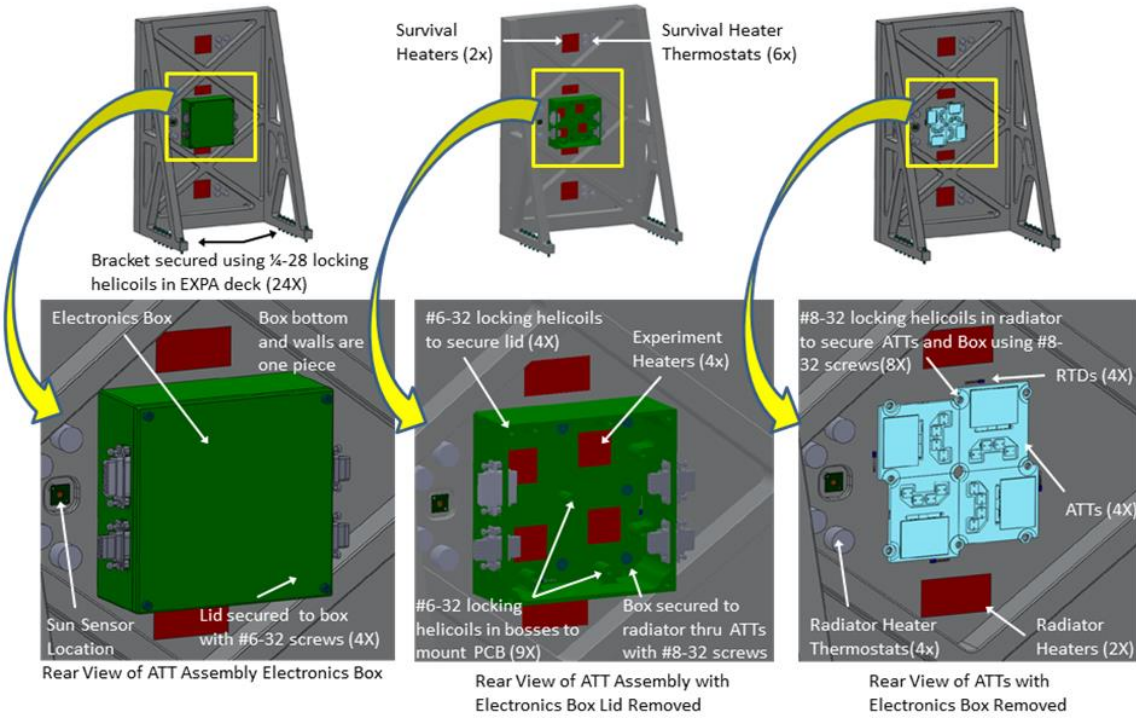

Figure 9: ATT experiment assembly (Williams and Hengeveld, 2011).

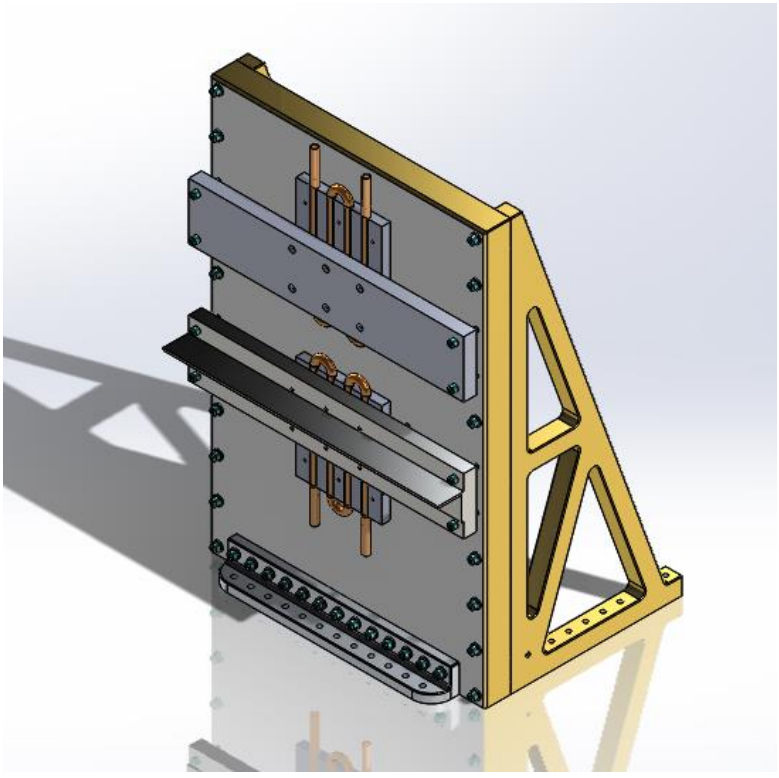

Figure 10: Cold plate mount configuration for tests.

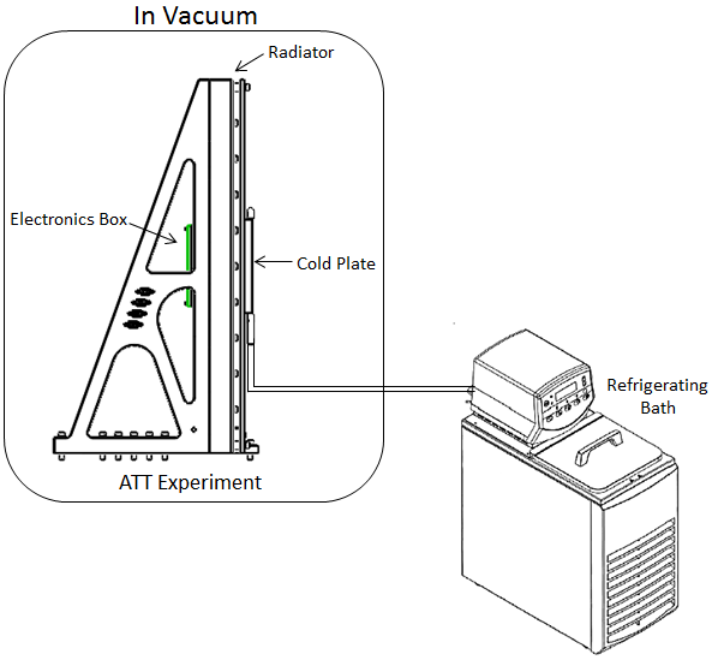

Figure 11: Setup for radiator cooling.

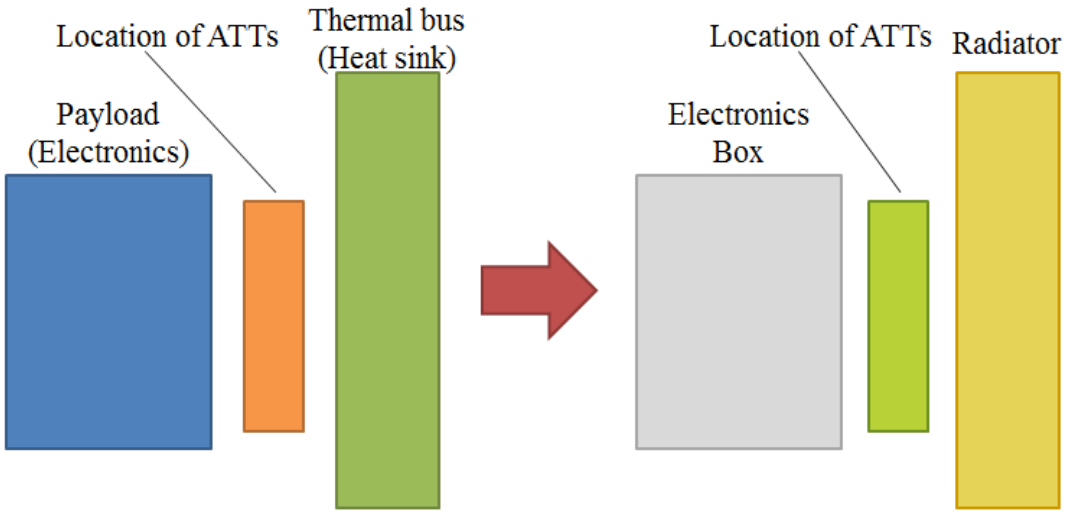

Figure 12: How the ATT experimental setup simulates a spacecraft.

2.2. Test Procedures

2.2.1. Cooling Cases

The ATTs were tested to determine their efficiency over a wide range of environments using the integrated software and a Windows HyperTerminal interface. By programming each of the cases shown in Figure 13 using HyperTerminal, the ATTs cooling ability and heating capability were measured, and their control structure was evaluated. First, their cooling ability was tested over 72 different variations of electronics box power, radiator temperature, and ATT current. Initial testing had been conducted on the two different units (flight and flight spare units) to verify the performance of both units. These results were compared to the current tests to assure nothing had changed and also to validate the chosen procedure yielded the desired results.

Radiator Temp [K]	ATT Current [A]	E-Box Heater Power [W]				
		5*	8	20	28	40
280	0.0	1	6	9	12	16
	0.6	2			13	
	1.0	3	7	10	14	17
	1.5	4			15	18
	2.0	5	8	11		
	2.5					
	3.0					

Radiator Temp [K]	ATT Current [A]	E-Box Heater Power [W]				
		5*	8	20	28	40
290	0.0	19	23	27	32	39
	0.6				33	
	1.0	20	24	28	34	40
	1.5			29	35	41
	2.0	21	25	30	36	42
	2.5				37	
	3.0	22	26	31	38	43

Radiator Temp [K]	ATT Current [A]	E-Box Heater Power [W]				
		5*	8	20	28	40
300	0.0	44	48	52	57	64
	0.6				58	
	1.0	45	49	53	59	65
	1.5			54	60	66
	2.0	46	50	55	61	67
	2.5				62	
	3.0	47	51	56	63	68

Radiator Temp [K]	ATT Current [A]	E-Box Heater Power [W]				
		5*	8	20	28	40
310	0.0				69	
	0.6					
	1.0				70	
	1.5					
	2.0				71	
	2.5					
	3.0				72	

Figure 13: Test matrices for cooling cases (Williams and Hengeveld, 2011).

There were three requirements for successful testing of a case: 1) the average composite radiator temperature must be within +/- 2K of the desired temperature setpoint, 2) less than 1K change in any component's temperature over an hour, and 3) electronics box power within 2% of the desired value. Initially, temperature was recorded every fifteen minutes to determine whether the experiment was at steady-state or not. After running four cases, it was determined that two hours was sufficient for the entire experiment to reach steady-state and maintain it for an hour. Thus, analysis was performed only on the last hour of data once the experiment had reached steady-state. The minimum temperature value during that hour was subtracted from the maximum temperature value found during that hour. This was to verify that the temperature did not spike or fluctuate excessively. To meet the requirement, this difference must be less than 1K.

HyperTerminal software offered the capability to set the ATT current and radiator temperature; however, setting the electronics box power was more complicated. The total power in the electronics box was made up of the electronics box heaters, which were set to run at a specific power, and the electronics control unit (ECU) which cannot directly measured.

Experiment power is distributed by two buses. Bus A controls the ECU inside the electronics box and the ATTs. Bus B controls both radiator and electronics box heaters. As the cooling cases were first being run, Bus A power was analyzed and compared to past tests in order to verify behavior. First, it was graphed over time to make sure it was constant. If those values remain constant throughout the hour the experimental setup was at steady-state and the average of those values could be taken and used for calculating

power values for the ATTs and electronics box. The graph showing the comparison between the validity tests and the ground tests for the first few cases run with a radiator temperature of 280K is shown in Figure 14 as an example of how Bus A power was examined.

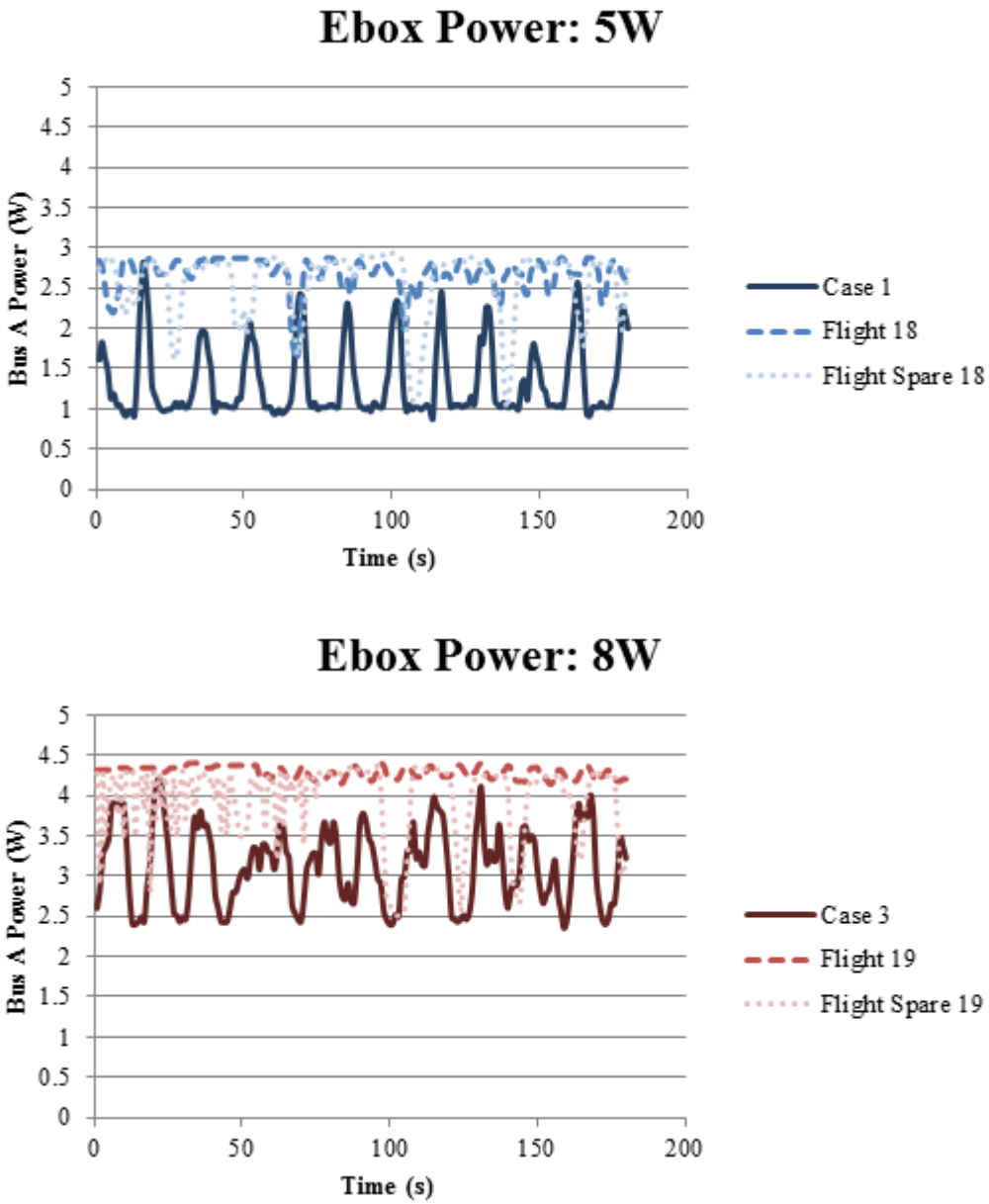

Figure 14: Bus A comparison for Cases 1 and 3 and the checkout testing from the previous year.

The fluctuating values shown in Figure 14 caused an error in the average value that was used to calculate the electronics box power – one of values used to determine success. The Bus A power waveform was graphed against other measured values to help determine this instability. A correlation between the electronics box heater duty cycle and Bus A power was discovered.

During testing, Bus A power was monitored, and heaters were individually switched on at full power. There was a notable decrease in Bus A power each time a heater was energized as shown in Figure 15. Bus A Power was then graphed versus heater duty cycle during an experimental case and a correlation was found. This is shown in Figure 16.

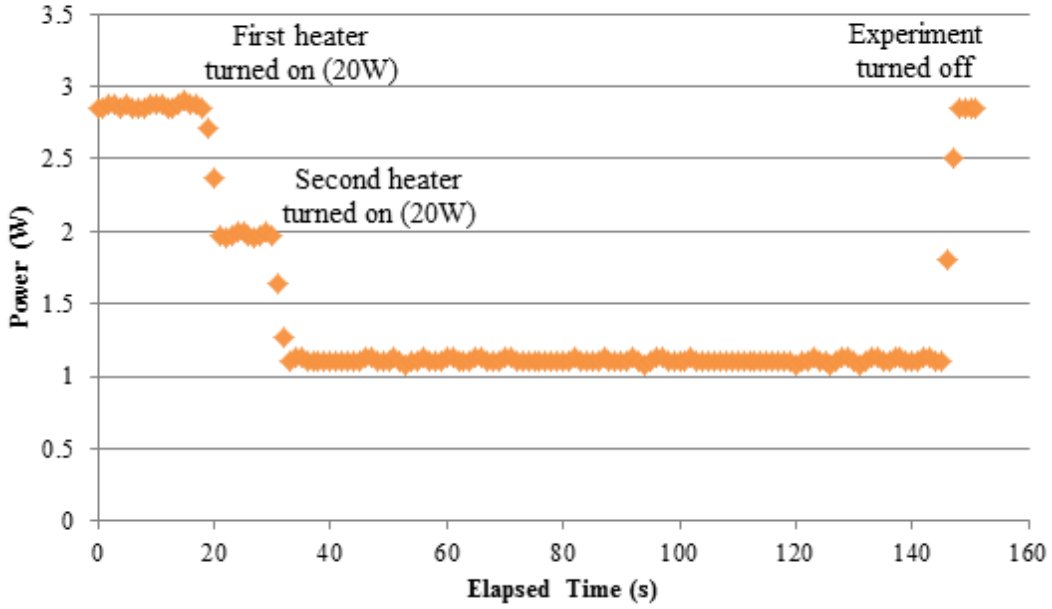

Figure 15: Bus A power versus time during troubleshooting.

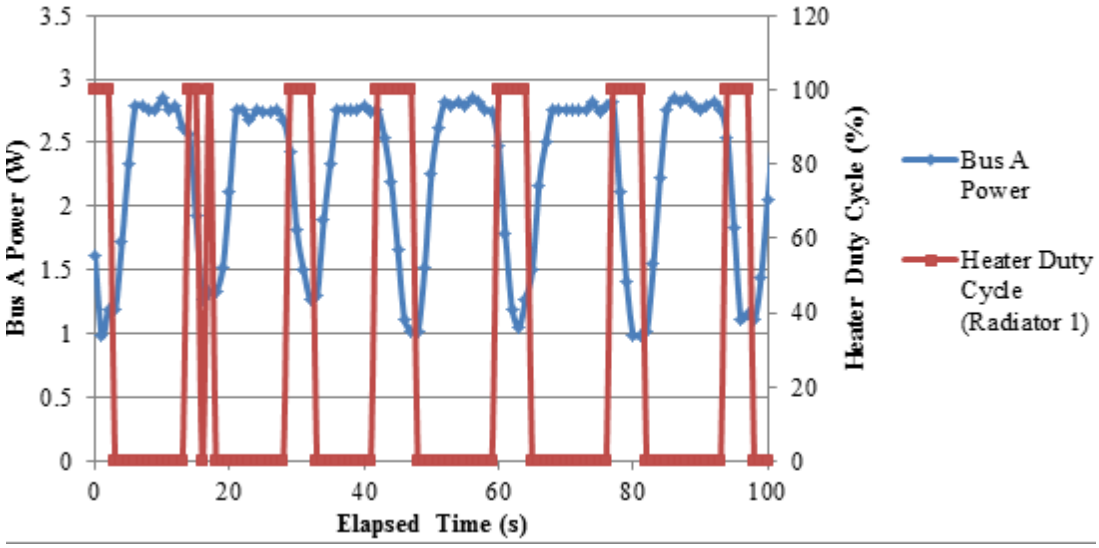

Figure 16: Bus A power versus heater duty cycle.

Bus A, which powers the ECU and ATTs, and Bus B, which powers the heaters, shared a ground. This meant that whenever the heaters would turn on, it would interfere with the Bus A measurement. Testing operations were modified to account for this anomaly. While running each case, another test would be run after the 2 hour experiment time duration had expired, and the experimental setup was at steady-state. At that point, the electronics box heaters would be shut off, while the radiator heaters and the ATTs would remain on for a three-minute time period. Data would be taken during this post-test, results were used to determine actual electronics box power.

Electronics box steady state temperature, radiator temperature, and Bus A power were then analyzed to determine test success. If unsuccessful, settings were altered and the case was re-run. Figure 17 is a flowchart depicting the process of running one case.

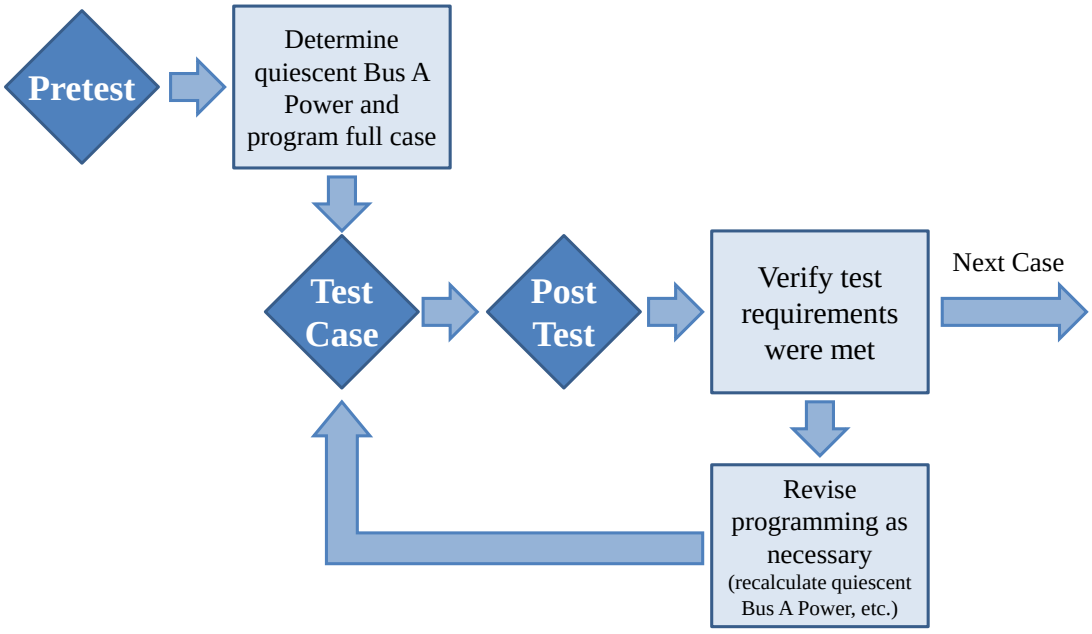

Figure 17: Flow chart describing test procedure.

After the post-test, parameters were set for the next case. Electronic box power was found using Equation (2.1) where $\dot{W}_E$ is the electronics box power, $\dot{W}_{BusA}$is the measured post-test Bus A power , $\dot{W}_{ATT}$ is the steady state test case ATT power draw, and $\dot{W}_{Htrs}$ is set heater power. All parameters are in watts.

$$\dot{W}_E = \dot{W}_{BusA} - \dot{W}_{ATT} + \dot{W}_{Htrs} \tag{2.1}$$

The files obtained from these tests are run through a Fortran data complier that transforms recorded data into labeled columns of test variables to be analyzed. ATT power, found by multiplying TED voltage and the TED current, is used with average Bus A Power to find the required power input to the electronics box heaters for test cases Equation (2.2).

$$\dot{W}_{Htrs} = \dot{W}_E - (\dot{W}_{BusA} - \dot{W}_{ATT}) \tag{2.2}$$

During test cases, the ATTs are programmed to run constantly by setting their target temperatures well below any temperatures that might be reached inside the chamber. The heater power found by Equation (2.2) is used to set the electronics box heaters. The target temperature of these heaters is set well above temperatures that might be reached inside the chamber to ensure they remain on during testing. Data collection begins, and the experiment is run until steady state is reached.

Once the cases were completed, the coefficient of performance (COP) was determined. The COP is the ratio of desired output to required input. This ratio is shown in Equation (2.3) where $\dot{Q}_E$ is the heat flow from the electronics box into the ATTs and $\dot{W}_{ATT}$ is ATT Power (Hengeveld, 2011).

$$COP_C = \frac{\dot{Q}_E}{\dot{W}_{ATT}} \tag{2.3}$$

ATT power is found by multiplying ATT voltage and ATT current, both collected during testing. Determining the heat flow from the electronics box into the ATTs is not as straightforward. The electronics box needs to be examined separately to determine where the work being put into the box is going. This is done in Figure 18.

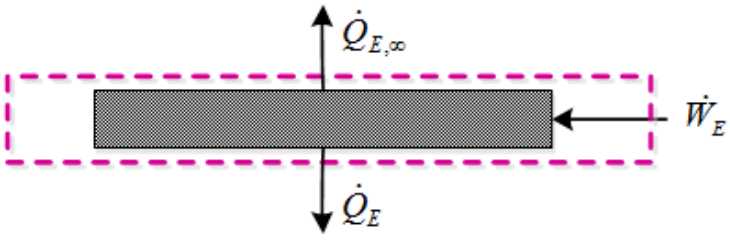

Figure 18: Heat transfer diagram of electronics box (Hengeveld, 2011).

As shown in Figure 18, there are only two ways for heat to be expelled across the boundary. It moves either into the surrounding environments or into the ATTs. The heat

transfer equation that represents the electronics box is shown as Equation (2.4) where $\dot{W}_E$ is the electronics box power and $\dot{Q}_{E,\infty}$ is the heat loss from the electronics box.

$$\dot{W}_E = \dot{Q}_E + \dot{Q}_{E,\infty} \tag{2.4}$$

Since the electronics box is highly insulated, it was assumed that $\dot{Q}_{E,\infty}$ is zero, which simplifies Equation (2.4). Equation (2.3) can then be stated as Equation (2.5) (Hengeveld, 2011) which was used to find ATT COP for the cooling cases.

$$COP_C = \frac{\dot{W}_E}{\dot{W}_{ATT}} \tag{2.5}$$

2.2.2. Heating Cases

Eight heating cases were run to explore the ATT's heating capabilities. Because of limitations in the test setup, ATT heating performance was determined by running equivalent cases with ATTs and with resistance heaters via four test cases, shown in Figure 19. Twelve cases were run: four cases used heaters to achieve test conditions, four used the ATTs running at 1.0A, and four used the ATTs running at 2.0A. The test matrices are shown in Figure 20.

Rad Temp [K]	Ebox Temp [K]		
	285	290	295
280			
290			

Figure 19: Basic test matrix for ATT Heating Cases.

Rad Temp [K]	Ebox Temp [K]		
	285	290	295
280	1	2	3
290			4

(A)

Rad Temp [K]	Ebox Temp [K]		
	285	290	295
280	5	6	7
290			8

(B)

Rad Temp [K]	Ebox Temp [K]		
	285	290	295
280	A	B	C
290			D

(C)

Figure 20: Heating cases test matrices. (A) 1.0A TED Cases; (B) 2.0A TED Cases; (C) Heater Cases.

For the cases using the ATTs, the radiator heaters were set using the HyperTerminal program, as well as the ATT current. The ATTs were run in a hysteresis style that would run the ATTs to keep them within a defined range of a set temperature. The range was set to be +/-0.1K. This was to mimic the on/off pattern the survival heaters follow when they are running.

To make the data comparable, the heaters needed to be run at as low of a power as necessary to reach the target temperature. Finding the proper heater power value that would give the desired result took some effort. The heaters were set in 2W increments from 6W to 40W. The experiment was set to reach 295K and to run at each power setting for two hours in order to reach steady state. A second heater sweep was conducted after that focused on power values that caused the electronics box steady state temperature to rest at the desired target temperatures in the initial heater sweep. Steady state temperatures were then graphed versus electronics box power. The results of this heater sweep are shown in Figure 21.

This analysis was done to find the minimum heater power necessary to meet test values. If the heaters never turned off during a test, it meant the target test temperature was never reached. If the heaters cycled excessively, too much power was being supplied to the electronics box that would result in an unfair comparison of the heater performance

to that of the ATTs. Therefore, the setting that would keep the heaters on and turn them off the least number of times, or the power setting that would maintain the target temperature and exceed it the least amount of times needed to be found. To find this power setting, heater duty cycle was graphed versus time and the setting that resulted in the graph that displayed the least amount dips in the waveform (but still some) was chosen. Figures 22 through 24 show the 280K radiator temperature cases, while Figure 25 shows the 290K radiator temperature cases. Table 1 summarizes the final values. Once values for the heaters had been chosen, the heating cases involving the electronics box heaters were completed.

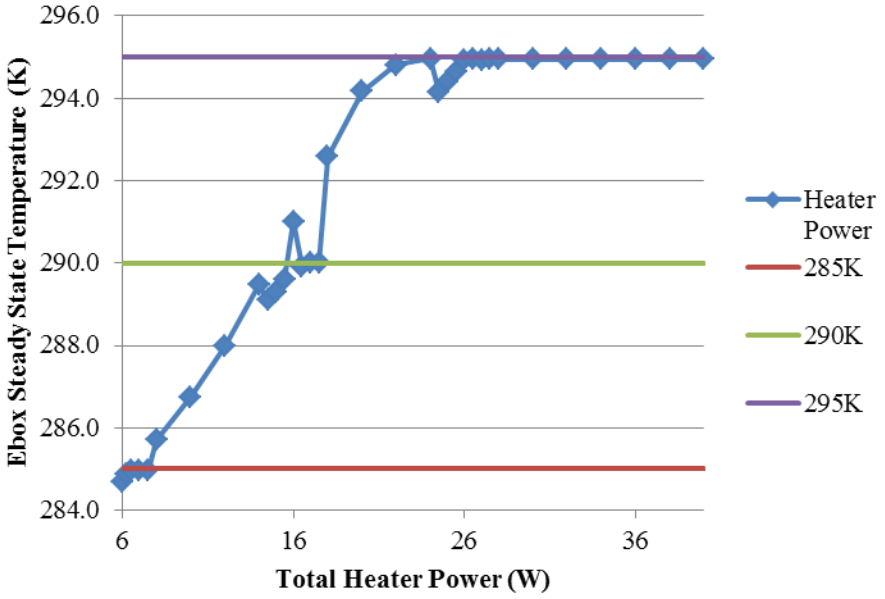

Figure 21: Heater sweep, with attention to between 6W and 8W for 285K, 14W and 18W for 290K, and 24W and 28W.

More examination was required for the case in Figure 22 because 6.50W still resulted in fluctuation in the duty cycle. The target temperature was not reached for the

6.25W and 6.38W tests, therefore they could not be used, and the 7.0W test heaters fluctuated between on and off too frequently.

Figure 23 shows that the target temperature was not reached for the 16W case, therefore it could not be used, and the 16.5W test heaters fluctuated between on and off too frequently meaning an excessive amount of power was being supplied to the electronics box to maintain the desired temperature.

Figure 24 shows that the target temperature was not reached for the 26W test, therefore it could not be used, and the 26.5W test heaters fluctuated between on and off too frequently.

Figure 25 shows that the target temperature was not reached for the 6.25W test, therefore it could not be used, and the 6.75W test heaters fluctuated between on and off too frequently. The fact that 6.5W was the value that resulted in the least amount of heater duty cycle fluctuations for this case and also for the 280K radiator temp/285K electronics box temperature case was particularly encouraging since both cases involve a 5K temperature differential.

The coefficient of performance needed to be found for the heating cases as well. The heat flow throughout the experiment is complicated with all the heating occurring in the electronics box. The cases needed to be analyzed slightly differently to compare ATT performance with heater performance. This is why the exact same tests were completed with the two different heating methods. COP can still be defined as the ratio of desired output to required input, which is represented by Equation (2.6) (Hengeveld, 2011), but instead of just looking at how much heat the ATTs move, the COP_H compares the power used to move heat using the heaters with the power used to move heat using the ATTs.

This equation is used with the assumption that the heater cases portray the nominal power needed to create a temperature differential.

$$COP_H = \frac{\dot{W}_{E_{Htrs}}}{\dot{W}_{E_{ATT}}} \tag{2.6}$$

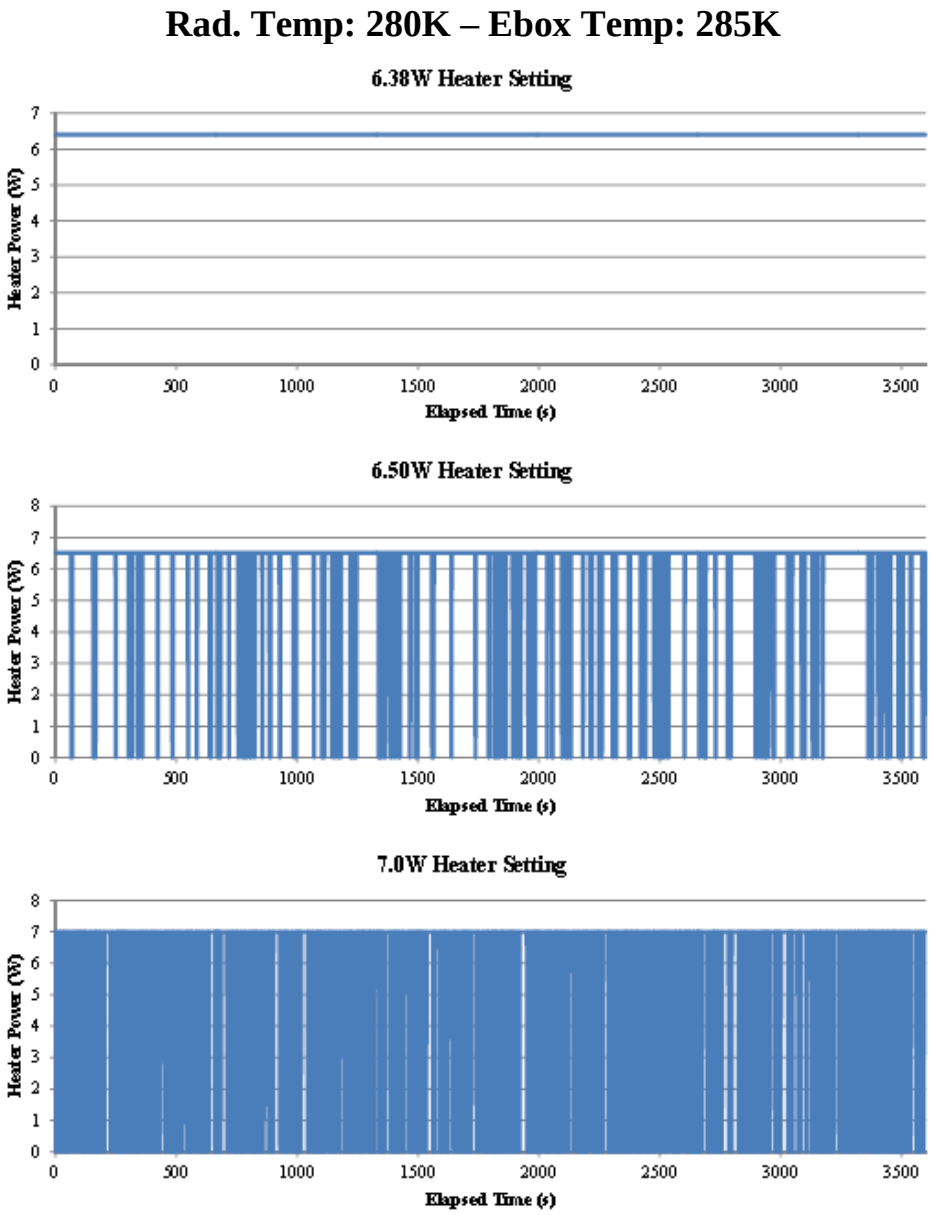

Figure 22: Heater power waveforms for several different heater settings with heater temperature setpoint of 285K and radiator temperature setpoint of 280K.

.

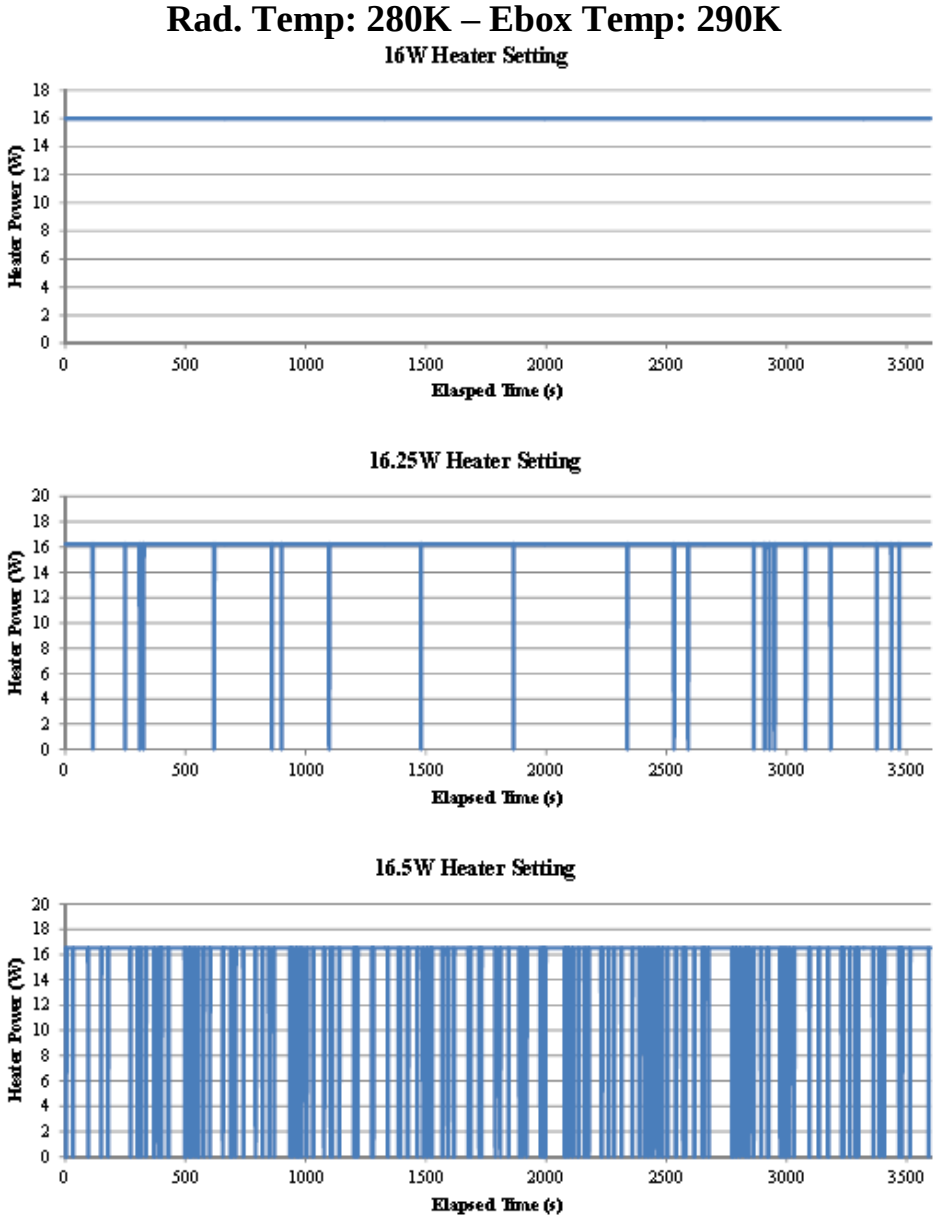

Figure 23: Heater power waveforms for several different heater settings with heater temperature setpoint of 290K and radiator temperature setpoint of 280K.

Rad. Temp: 280K – Ebox Temp: 295K

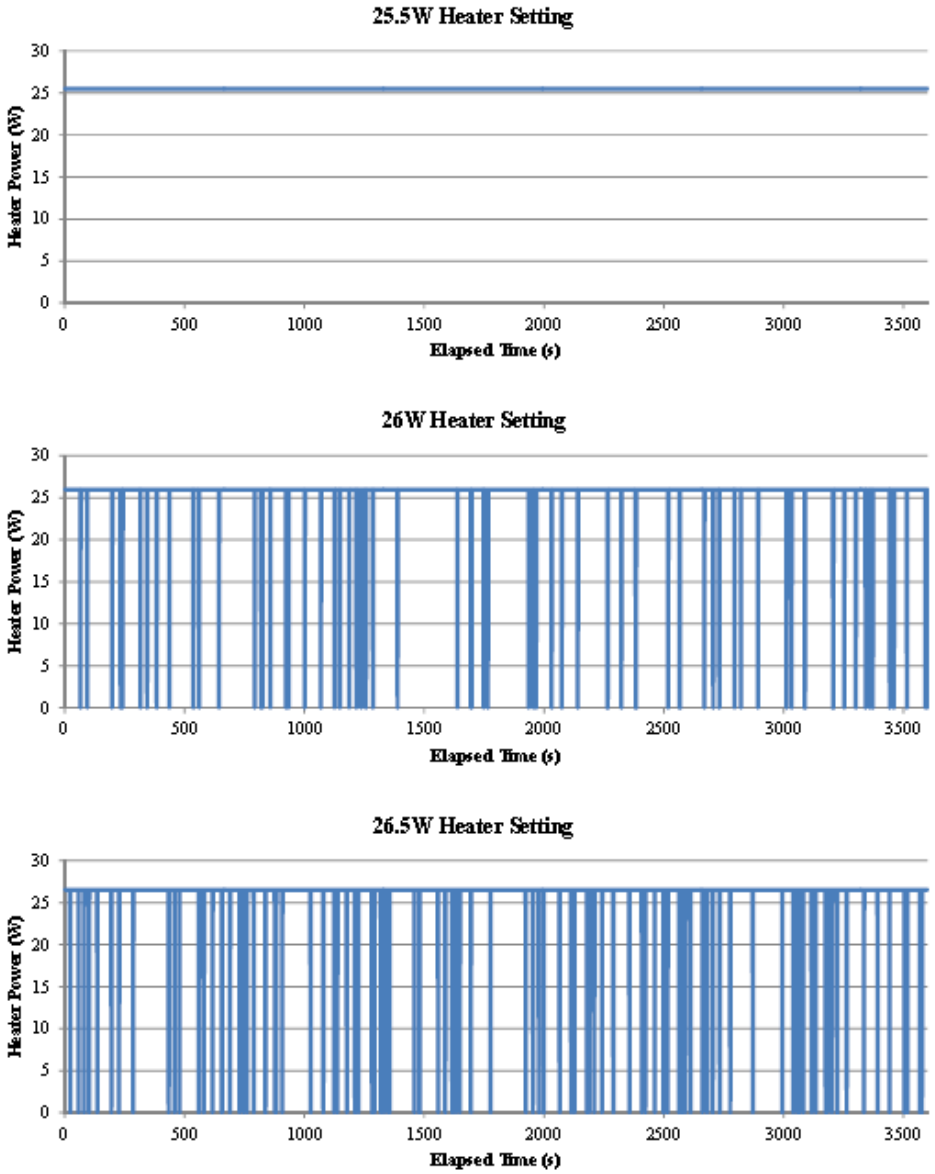

Figure 24: Heater power waveforms for several different heater settings with heater temperature setpoint of 295K and radiator temperature setpoint of 280K.

Rad Temp: 290K – Ebox Temp: 295K

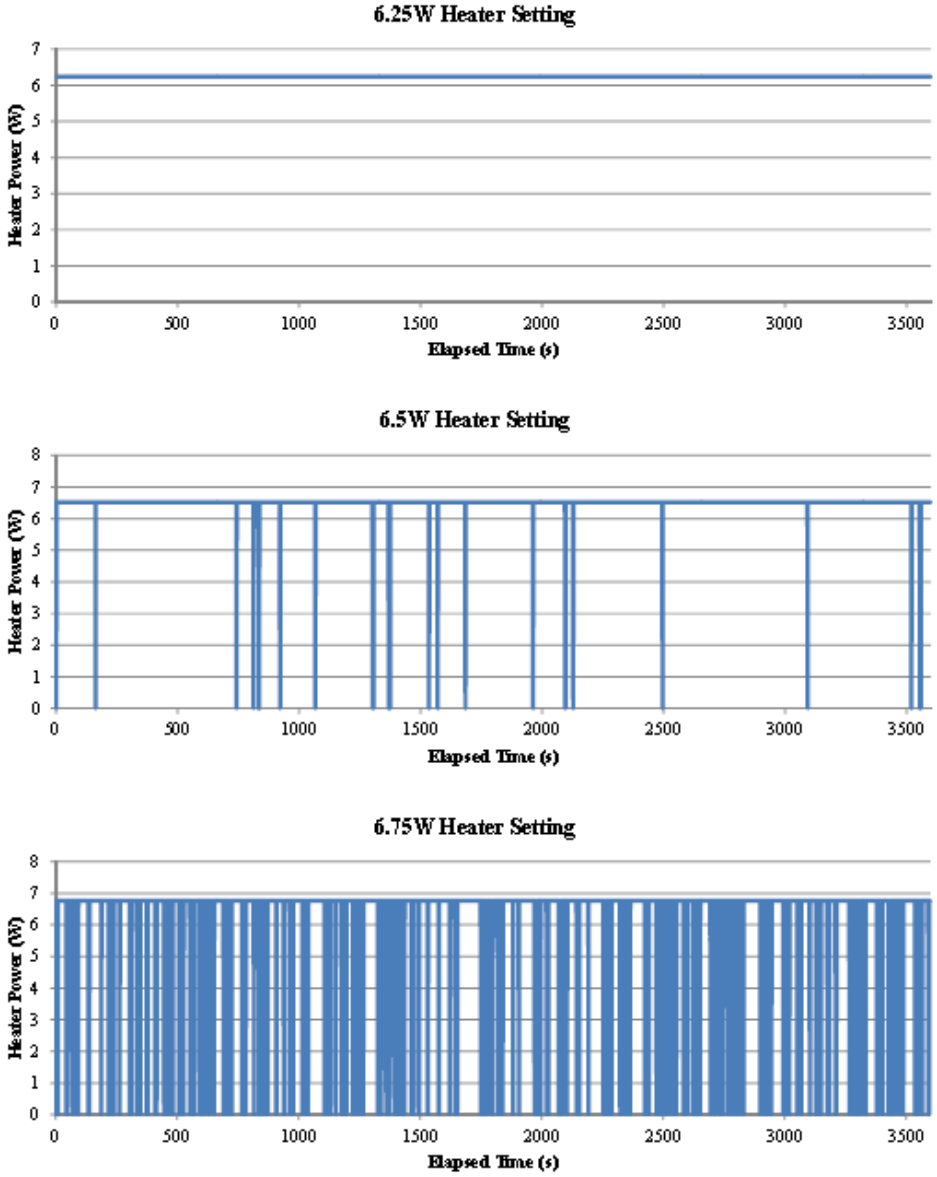

Figure 25: Heater power waveforms for several different heater settings with heater temperature setpoint of 295K and radiator temperature setpoint of 290K.

Table 1: Final heater power values.

Radiator Temp: 280K	
Ebox Temp	Total Heater Power
285K	6.52W
290K	16.24W
295K	26.00W

Radiator Temp: 290K	
Ebox Temp	Total Heater Power
295K	6.52W

3. Results and Conclusions-Performance Tests

3.1. Comparing Ground Tests with Past Tests

Before any data analysis could be done, the tests needed to be checked to determine if they met the requirements for a successful test. These requirements include the radiator being within 2K of the setpoint, less than 1K change in temperature over an hour for both the radiator and the electronics box, and the electronics box power within 2% of the desired value.

First, the data from the ground tests were compared with data taken the year prior. This was done to make sure that nothing had changed since the past year. The prior tests, termed validity tests, confirmed that the flight spare and the flight unit maintained performance levels and were comparable. It was essential that the flight spare still performed the way it had the year before in order to compare it to the performance of the flight unit. If not, the data collected from the flight spare unit could not be compared with the data collected from the flight unit on-orbit.

The electronics box temperature was graphed over time. This was to make sure the experiment reached steady-state and did not fluctuate over time. An example of how the temperature was checked for each set of cases per radiator temperature for both the validity and the ground tests is shown in Table 2.

Table 2: Electronics box steady state temperature versus time for 280K validity cases performed the previous year compared to the ground tests.

Ebox Power [W]	ATT Current [A]	Ebox Temperature [K]				
		Present Case	Flight Unit	% Diff	Flight Spare	%Diff
5W	0.0A	282.8K	282.8	0.00%	283.0	-0.07%
5W	1.0A	276.5K	276.4	0.04%	276.4	0.04%
8W	0.0A	284.2K	285.2	-0.35%	284.2	0.00%
8W	1.0A	278.5K	279.6	-0.39%	278	0.18%

The steady-state electronics box temperature with regard to ATT current was also studied. It needed to be verified that both the flight and flight spare units achieved similar steady-state temperatures during their tests. The graphs showing the comparison between the validity tests and the ground tests are shown in Figure 26.

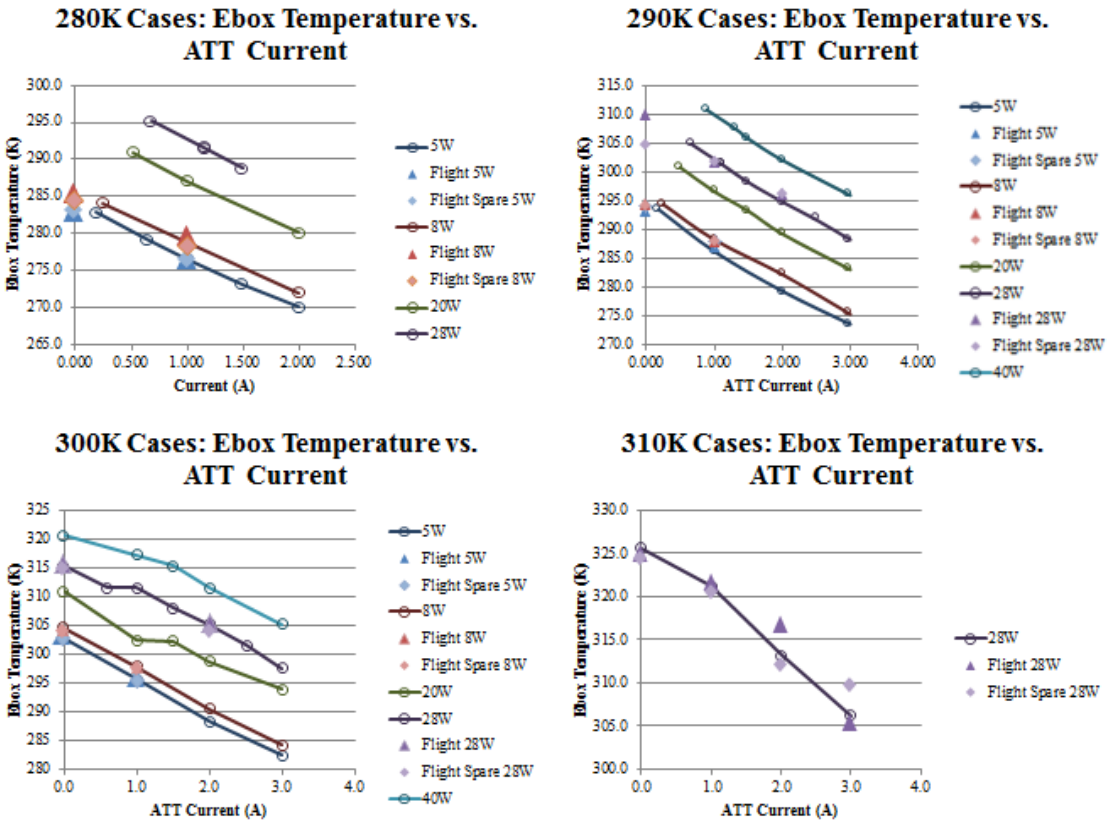

Figure 26: Flight-Flight Spare Validity Tests versus Present Tests final electronics box temperature comparison.

Lastly, the coefficients of performance (COPs) at each radiator temperature and ATT current were compared for both the present cases and the validity tests. The validity test COPs and their percent differences from the present cases are shown in Table 3. The percent differences vary from -1.18% to 28.19%. The relatively high percent difference is because the heater powers for the past work differed from the desired value more than those of the present cases because of the requirements for a successful test being so tight. The validity tests were conducted under less strict requirements. COP is dependent on those heater power values, so if it varies, the COP will also change.

Table 3: Flight-Flight Spare-Ground Test performance comparison.

Rad. Temp [K]	Ebox Power [W]	ATT Current [A]	Coefficient of Performance				
			Present Case	Flight Unit	% Diff	Flight Spare	%Diff
280	5	1.0	4.607	4.345	5.69%	4.340	5.81%
	8	1.0	8.101	7.827	3.39%	7.422	8.39%
290	5	1.0	4.310	3.716	13.80%	3.779	12.33%
	8	1.0	7.528	6.645	11.73%	6.491	13.78%
	28	1.0	43.031	43.797	-1.78%	43.810	-1.81%
	28	2.0	7.568	7.942	-4.94%	7.044	6.93%
300	5	1.0	4.178	3.000	28.19%	3.041	27.21%
	8	1.0	7.143	6.063	15.13%	5.879	17.69%
	28	2.0	7.023	7.105	-1.18%	7.361	-4.18%
310	28	1.0	46.029	43.339	5.85%	40.771	11.42%
	28	2.0	6.700	6.363	5.02%	6.2673	6.51%
	28	3.0	2.643	2.518	4.71%	2.480	6.17%

The average percent differences between the validity test values and the ground test values are shown in Table 4. The percent difference in the electronics box temperature is small, but there are significant differences in ATT Power and COP.

Table 4: Average percent differences between validity tests and ground tests.

	Flight			Flight Spare		
Rad. Temp	Average % Difference in Ebox Temp	Average % Difference in ATT Power	Average % Difference in COP	Average % Difference in Ebox Temp	Average % Difference in ATT Power	Average % Difference in COP
280K	-0.24%	-0.90%	4.54%	0.07%	-1.05%	7.10%
290K	-0.17%	-0.76%	4.70%	0.16%	-0.95%	7.81%
300K	-0.01%	0.38%	14.05%	0.10%	-0.53%	13.36%
310K	-0.25%	-1.14%	5.19%	-0.08%	-4.74%	8.03%

Table 4 shows the electronics box temperature from the most recent tests varies by less than 1% from the previous tests, and the average ATT power varied by less than 5% which shows that the setup performed nearly the same as it had previously, so the data collected on the ground could still be compared to the data collected on-orbit.

The large COP differences can be attributed to the tight requirements on electronics box power for the current cases that did not exist when the initial testing was completed. Since that was the case, the difference between the actual and desired electronics box powers was larger for the past cases, which caused different COPs and a large percent difference between the two.

3.2. Cooling Case Performance

The performance of the ATTs was examined in two ways. The first method examined the ATTs performance with respect to the entire experiment. In this analysis, the final composite temperature of the electronics was subtracted from the composite temperature of the radiator. This temperature difference versus ATT current is shown in Figure 27. As expected, each power setting presented a similar response. As ATT current increases, temperature difference decreases at a rate of around 7K per amp. These figures also show how an increase in electronics box power affects performance. The greater the

electronics box power, the more current the ATTs must use to make a large impact by cooling, and therefore, the greater the positive temperature differential of the experiment. Vice versa, the less power supplied to the heaters, the less current is needed for the ATTs to make an impact. This data was compared to the performance curves provided by Marlow Industries, the manufacturers of the TEDs used in the ATTs, as shown in Figure 28. The figures are similar, while the values differ. This is because there is more than one ATT being used on this setup which would cause the experiment to create a higher temperature differential while using a lower ATT current.

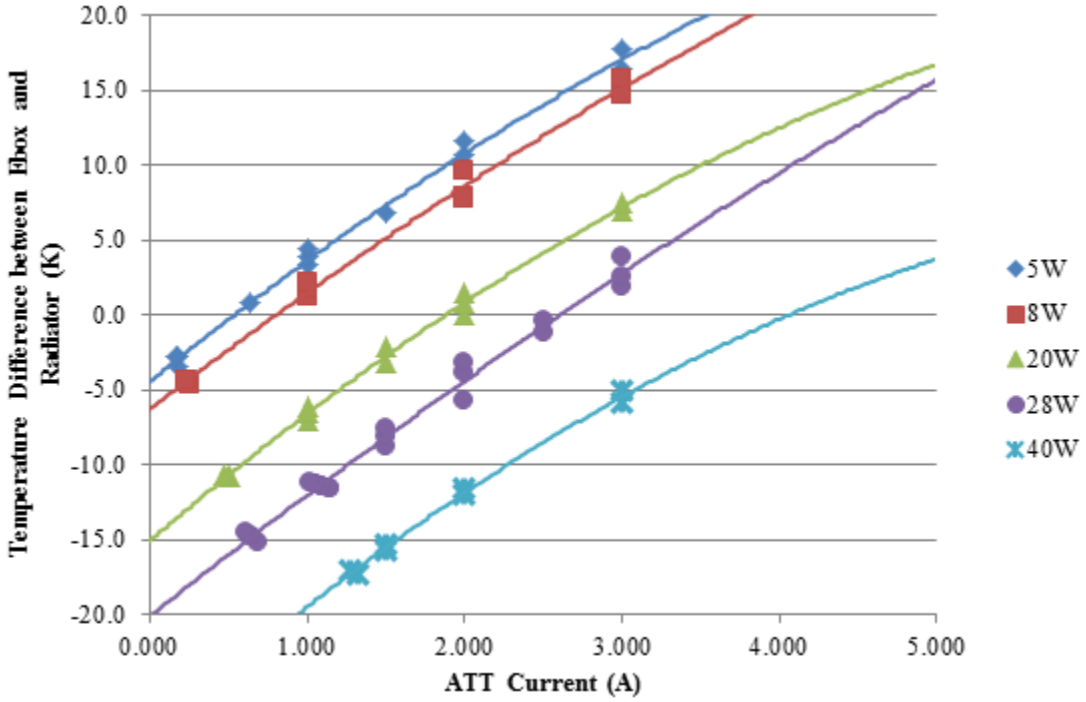

Figure 27: ATT experiment performance map (The temperature differential created by subtracting electronics box steady state temperature from the radiator steady state temperature vs. ATT current).

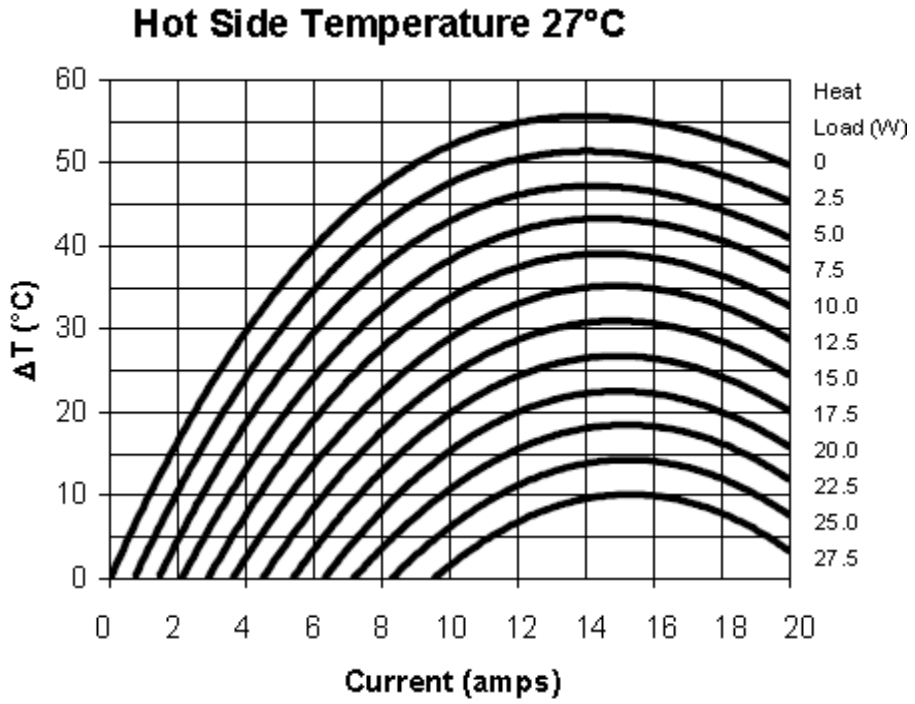

Figure 28: Marlow TED performance (Technical Data Sheet: XLT2391 Single-Stage Thermoelectric Cooler).

The relationship between ATT power and change in electronics box temperature was also examined. When designing a spacecraft, the amount of power used to create a temperature gradient must be known. ATT power and change in electronics box temperature create a parabolic curve. This is because as current flows through the ATTs, heat is generated, and the ATTs have to use more power to remove more heat. These curves, shown in Figure 29, are also similar to those from experiments by Wang (2007) and Ramanathan and Chrysler (2006).

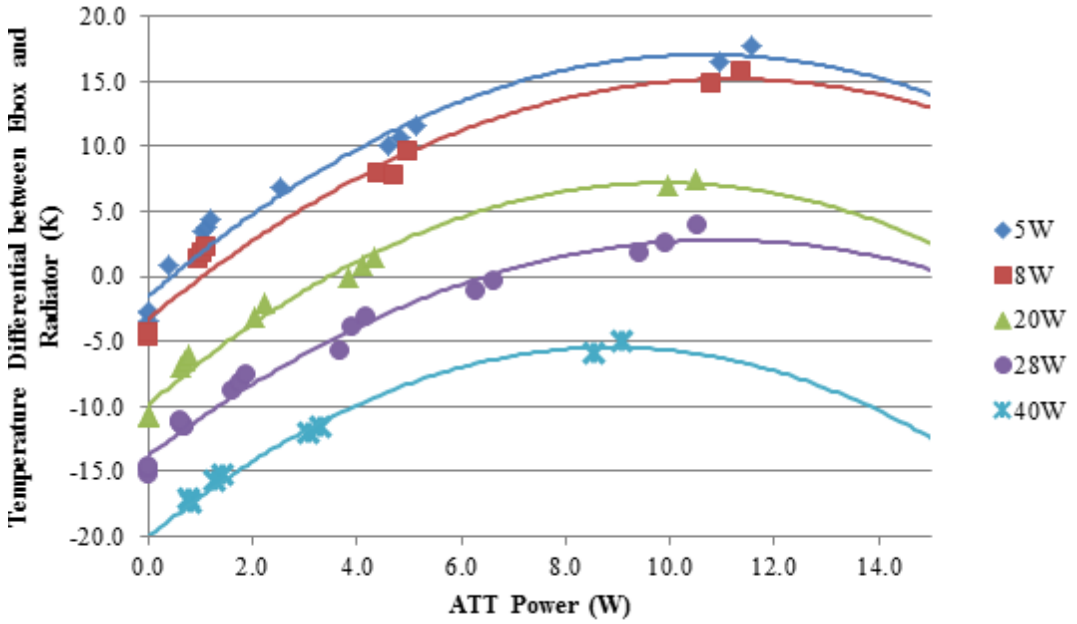

Figure 29: ATT experiment performance map (Temperature differential found by subtracting radiator steady state temperature from the electronics box steady state temperature vs. ATT power).

3.3. Heating Case Performance

New analysis methods were introduced for the heating cases. Like the cooling cases, the second hour of each test was selected for analysis. The first step in analyzing the data collected from the heating cases was to make sure the target temperature was reached. Case 4, which required the ATTs to create a temperature differential of 15K, failed to reach its target temperature, so it was omitted. However, it can then be concluded that 1.0A is not a large enough current in heating mode to maintain a 15K temperature differential between the payload and the radiator.

The next step was to analyze the difference in power usage for each temperature differential. Figure 30 shows the waveforms for the smallest temperature differential. The power for only 200 seconds is shown to give a better idea of the details of the waveform. One can notice both the ATTs and the heaters cycling on and off, but the ATT

waveforms are more rounded and periodic. The heaters' waveform is much more sporadic. The difference can be explained by the software: the program only checks the current (amp) value to adjust the voltage value every three seconds. Also, there is a limit to how high the voltage can instantaneously rise: the limit is 1.0V corresponding to 1.0A for the four ATTs in series. When TED current is supposed to rise to 2.0A, it will only do so in 1.0A increments every 3 seconds.

Figure 31 shows waveforms for the cases with a 10K temperature differential. As expected, the peaks in ATT power have the same amplitude but are wider than in the 5K temperature differential plots. This is because the ATTs, while running at the same currents, need to heat longer to maintain the larger temperature differential.

Figure 32 shows the 15K differential heating case. The case using a TED current of 1.0A to maintain a 15K temperature differential failed to reach the target temperature. The 1.0A waveform shows that the ATTs were constantly on. This means they never were able to reach their target temperature and therefore never turned off. The 2.0A waveform, once again shows wider peaks than in the previous two plots.

COP was examined for the heating cases as well. Cases using ATTs to heat the electronics box (numbered cases) were compared to correlating cases which use heaters to heat the electronics box (lettered cases). Thus, cases 1 and 5 were compared to Case A, Cases 2 and 6 were compared to Case B, Case 7 was compared to Case C, and Cases 4 and 8 were compared to Case D.

An increase in COP can be seen with the increase in temperature differential. This is because these COPs are not traditional COPs. In these cases, the COP is a measure of comparison between heaters and the ATTs. Figure 33 shows the correlation between

power usage and temperature differential for both the heaters and the ATTs. While both slopes show that power usage increases with increasing temperature differential, the slope formed by the heater cases is much steeper, meaning more power is needed to create a larger temperature differential with the heaters than is needed to create the same temperature differential with the ATTS. Since COP is a comparison of the power required by the heaters relative to that required by the ATTs, it is related to the increasing distance between the two trend lines in Figure 33. Therefore, COP should increase with the increasing temperature differential.

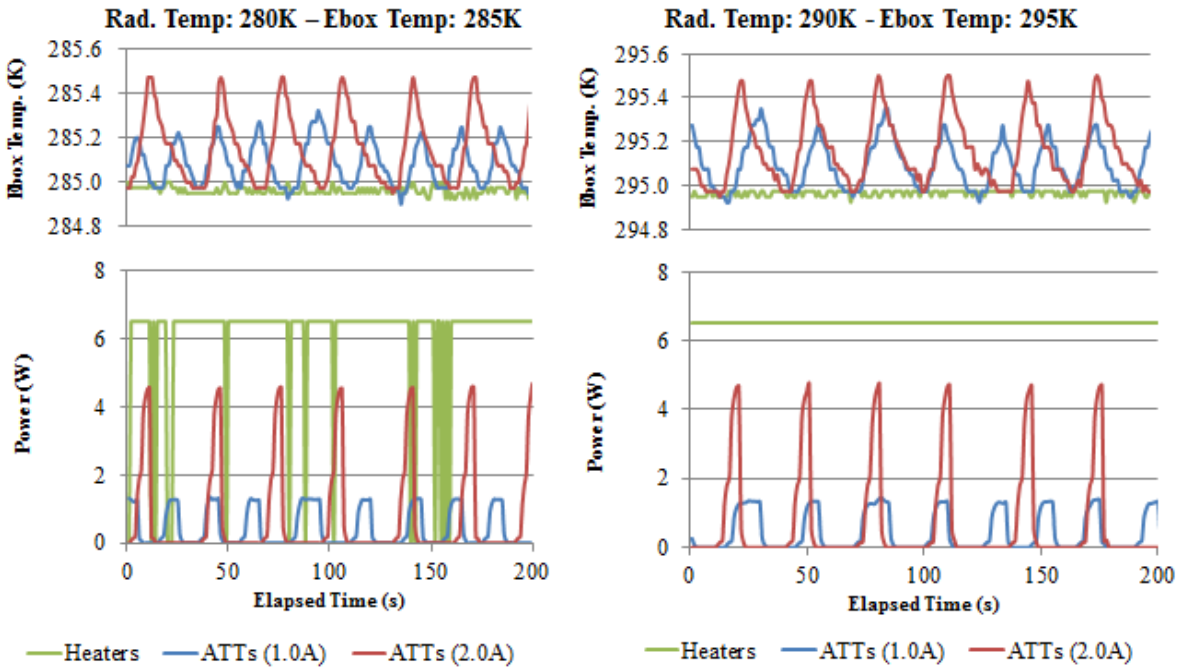

Figure 30: ATTs power and electronics box temperature versus time waveforms for 5K temperature differential.

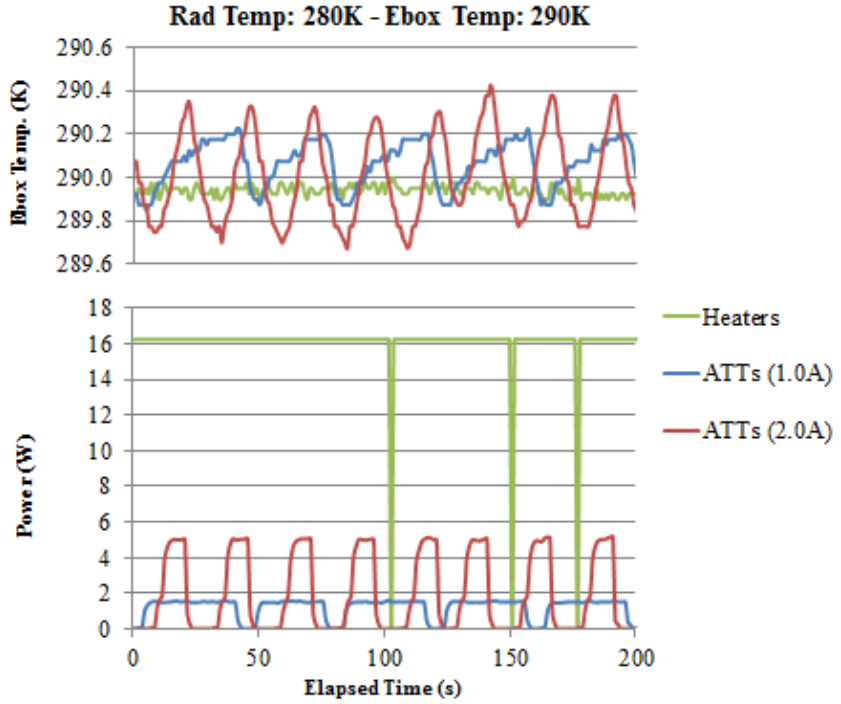

Figure 31: ATTs power and electronics box temperature versus time waveforms for 10K temperature differential.

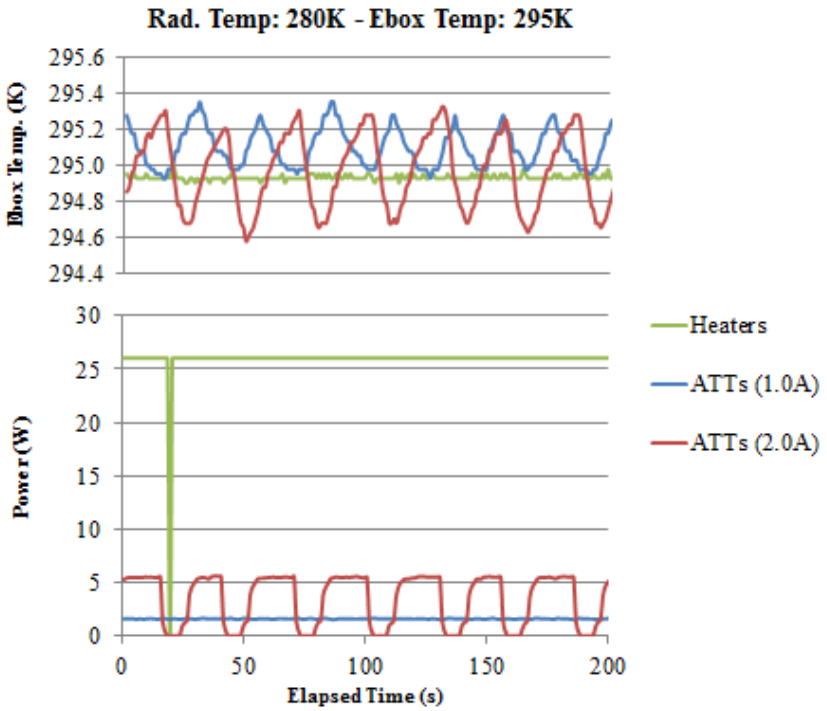

Figure 32: ATTs power and electronics box temperature versus time waveforms for 15K temperature differential.

Table 5: COP for each heating case.

ATT Curr. (A)	Rad. Temp (K)	Ebox Temp (K)	COP
1.0	280	285	2.511
	280	290	4.113
	280	295	---
	290	295	2.521
2.0	280	285	2.358
	280	290	3.307
	280	295	3.847
	290	295	2.343

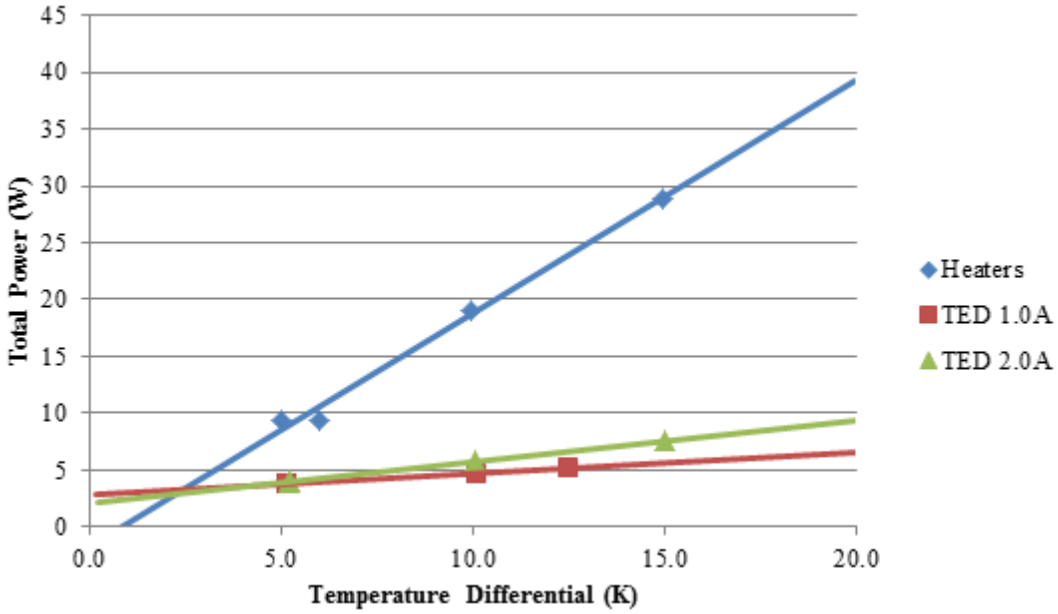

Figure 33: Power usage versus temperature differential between electronics box and the radiator.

3.4. Uncertainty Analysis

Standard deviation and resolution of values being collected were used to determine the standard Type B uncertainty of the measurements and calculations made. A normal distribution was used. Overall the measurement uncertainty was less than +/3%.

The exception to this is the Bus A and Bus B values which had significant error because of the ground loop in the design. These values are shown in Table 6.

Table 6: Uncertainty of measured and calculated values for performance tests.

Measured		**Calculated**	
Value	**% Uncertainty**	**Value**	**% Uncertainty**
Radiator Temp	±0.04%	Bus A Power	±2.09%
Ebox Temp	±0.04%	Bus B Power	±54.42%
ATT Current	±0.96%	ATT Power	±1.15%
ATT Voltage	±0.63%	ECU Power	±2.38%
Bus A Voltage	±0.25%	Total Ebox Power	±54.47%
Bus A Current	±2.08%	COP_C	±54.49%
Bus B Voltage	±0.75%	COP_H	±54.49%
Bus B Current	±54.42%	ATT Energy	±1.15%
		ATT Resistance	±1.77%

4. Experimental Method – Controls Testing

The Active Thermal Tiles (ATTs) could be controlled in two ways: a proportional-integral-derivative (PID) controller or an On-Off controller. A PID controller uses proportional, integral, and derivative constants to adjust ATT current to meet and maintain a target temperature while keeping the ATTs constantly on. An On-Off controller cycles the ATTs on and off to maintain the target temperature. These two control methods were compared to determine which uses the least amount of energy. Before that comparison could be made, the PID constants needed to be found.

Since PID constants are usually found by a trial and error method, the same cases would have to be run while varying the constants until the ATTs ran the most efficiently. Each ground test takes at least two hours to complete. However, the developers of the ATTs, Infoscitex, wrote a program that would simulate the ATT experiment once the proper initial conditions were input. This program could also run in a PID controlled mode. With this program, a two-hour long experiment could then be shortened to three minutes so more constants could be tested per day. Hence, the control program was a much more effective way of finding the most efficient ATT PID constants.

The intent of these experiments was to determine which method causes the ATTs to keep the electrical component at a set temperature while using the least amount of energy. Both of these methods were tested under -5K and -10K temperature differentials since those were the cases that would be most greatly impacted by the two different experimental methods. These are the greatest temperature differences achieved using ATT currents less than 3.0A.

The first step was to make sure the control program was tuned well enough to match test data. The initial conditions were input, and the geometry and material properties of the setup were programmed. There were other unknown factors that could be manipulated to tune the program. These factors include the interface resistance between aluminum and the ATTs, the multiplier for the TED resistance, the multiplier for the thermoelectric coefficient, and the multiplier for the aluminum thermal capacity. Each factor was adjusted to create resulting waveforms that matched the test values within +/- 5% of test values. Examples of the how each factor adjusted the behavior of the control simulation are shown in Figure 35. The various dash lines represent the different variations of each factor, while the solid lines represent the original ground data that the simulation should be tuned to match.

Once that was completed, the program was set up to be controlled by the PID controller. Since the system being controlled is thermal and running until a steady-state, a proportional controller should be all that is necessary. The program was then tuned to find the proper proportional gain needed to maintain a set temperature while using the least amount of energy possible. The program was run multiple times, each time varying the proportional gain until the gain was too large to maintain a steady temperature. The proportional constant was then scaled back just enough to result in a fixed temperature at steady-state.

The On-Off method was simulated by raising the gain exceedingly high. The program used only had PID control available; however, when the gain is set too high, the ATTs will turn on at full power, and turn off again when the target temperature has been

met. The gain was set to 10000 for the ground checkout tests, so that is what the gain was set to for the On-Off method in the simulation.

After the tuning of the program and simulating the different run modes, the values for the proportional gain for each of the selected cases were obtained by running the six cases over and over while varying the gain until the largest gain that resulted in the system converging on the temperature closest to the target was found. Then, the cases were run on the experimental setup inside the vacuum chamber using the same parameters as were programmed into the simulator, and the results were compared to the results of the program.

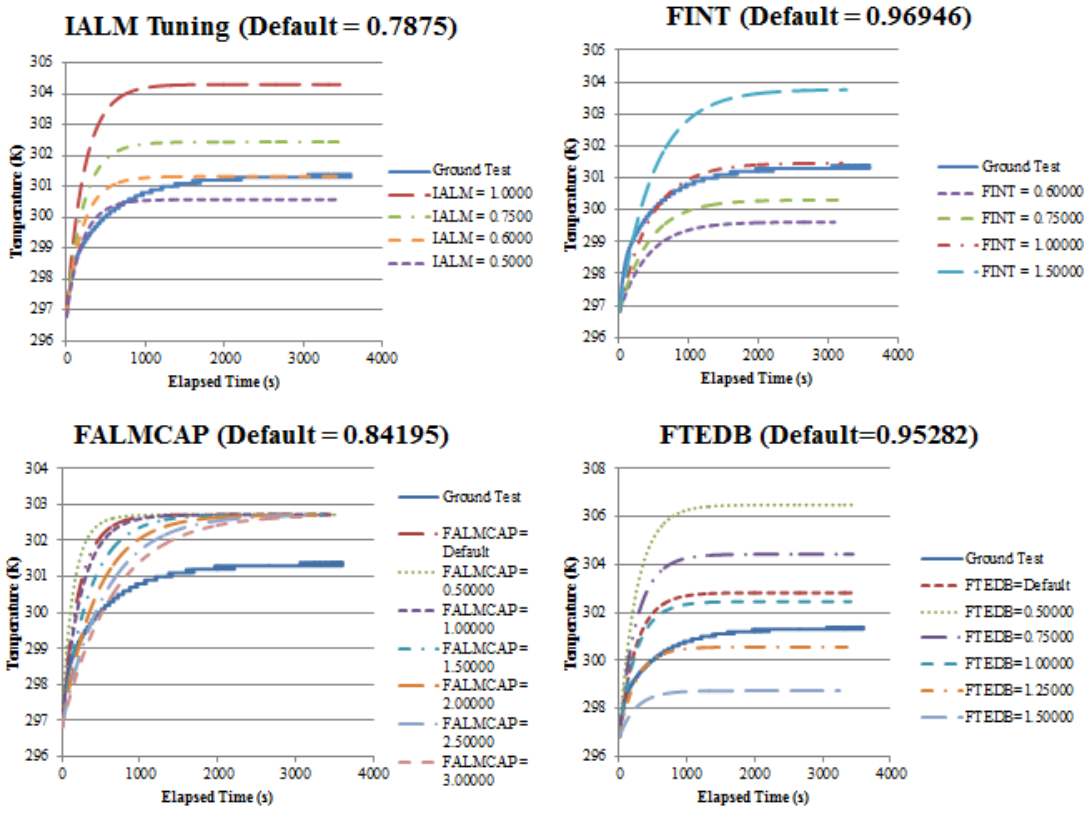

Figure 34: Effects of four different factors on the control simulation results. IALM = Interface resistance of aluminum; FINT = multiplier for interface resistance; FALMCAP = multiplier for aluminum thermal capacity; FTEDB = multiplier for the thermoelectric coefficient.

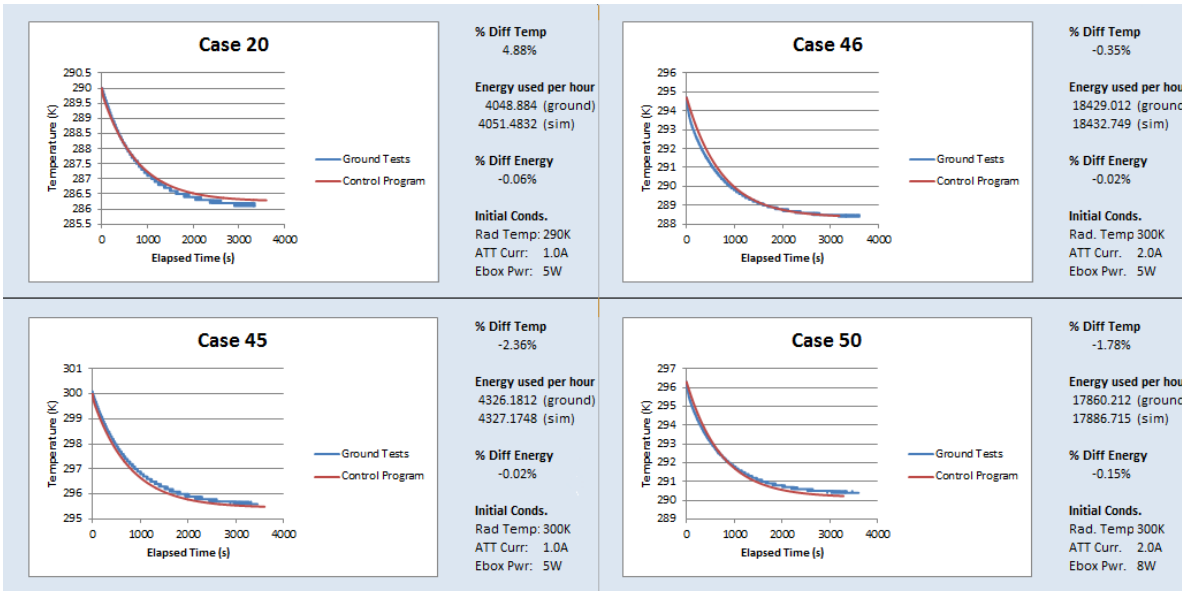

Figure 35: Examples of control program tuning.

5. Results and Conclusions – Controls Testing

5.1. Simulation Results

First, the six cases were tuned to match the test data. This was done using the defaults from the given control program and adjusting four of the variables. Each case was done separately, and the results of the tuning are shown in Figure 36. All of the cases were tuned so the results of the simulation were less than +/-5% different than those from the ground tests.

Once the program was tuned to match the test data, the PID constants were found for each of the cases. This was done by increasing the proportional gain in the program until the system ceased to converge to a temperature. Then the gain was scaled back so that it resulted in a waveform that converged on a temperature while requiring the smallest amount of current. The gains for these cases are shown in Table 7. Once those gains were found, the simulation was run in its control mode using those gain values, and then again with the gain set to 10000 A/K to simulate an On-Off mode.

The results of the three different types of simulations are shown in Figures 37 through 42. Each figure shows ATT current as well as electronics box temperature versus time. The top graphs show both the simulation and the original performance test for each particular case. This simulation was run with a constant ATT current until the experiment had reached steady state. The middle graph shows the performance of the simulation when controlled by the gains shown in Table 7. The currents in these graphs fluctuate before settling on a steady current. The bottom graph shows the performance of the simulation when it is controlled by an On-Off control method. In these graphs, the current

fluctuates between 0.0A and 3.0A (the limit the ground unit software imposes on ATT current) during the simulation to maintain the set temperature.

Final temperature, average current, and total energy over an hour were all noted in order to compare the two control methods. Table 8 shows the comparison between the initial performance test data and the simulation results. The energy values for each of the PID controlled cases were proportional to TED current: this matched expectations since energy is the integral of power over time, and power is proportional to current. The currents in the PID cases also were within 3.5% of the TED current values used for the original cooling cases. The original cases reached their final temperatures by constantly running the TEDs at certain currents. The average currents of the PID controlled program would end up being similar to those from the ground tests. The On-Off controlled method was different. While final temperatures hovered around the proper target temperature, the energies and currents of the on/off tests remain close to the same value regardless of the temperature differential.

Figure 43 is shown as an example of the difference between the PID controlled cases and the On-Off controlled cases. The figure shows power versus time with energy being the integral of power over time. According to the simulation, the PID controlled cases are up to seven times more efficient than the On-Off cases. The actual percent differences in energy usage are shown in Table 9. These were calculated by dividing the difference between the energies from the two different methods by the energy usage during the PID tests. It is not known why the powers for the simulated On-Off cases differed so much from the simulated ground tests.

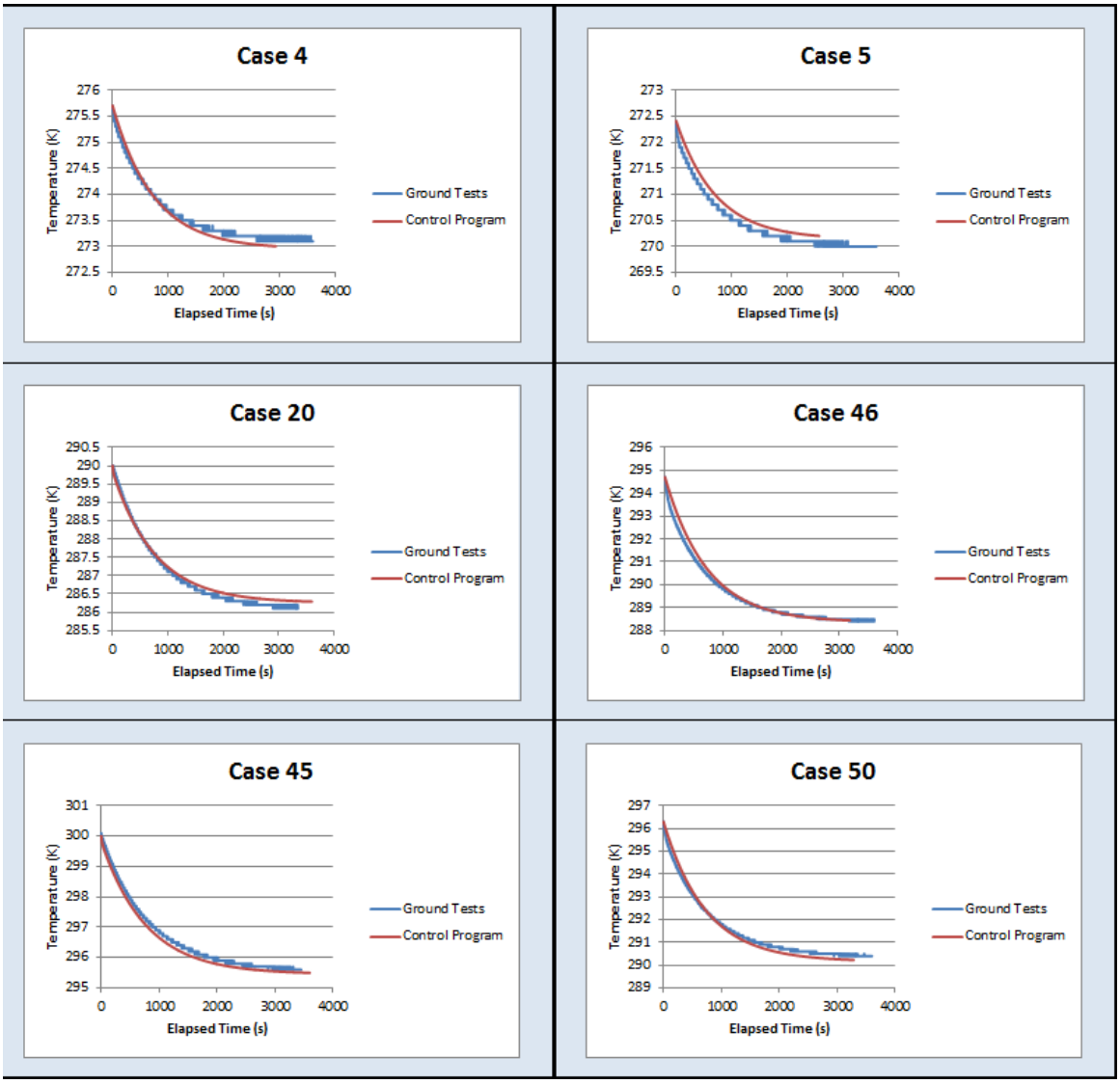

Figure 36: Control program cases tuned to ground tests. The cases on the left have a -5K temperature differential, while the cases on the right have a -10K temperature differential.

Table 7: Gains for the six simulated test cases.

ΔT	Case	Gain (A/K)
-5K	**4**	611
	20	650
	45	679
-10K	**5**	662
	46	692
	50	739

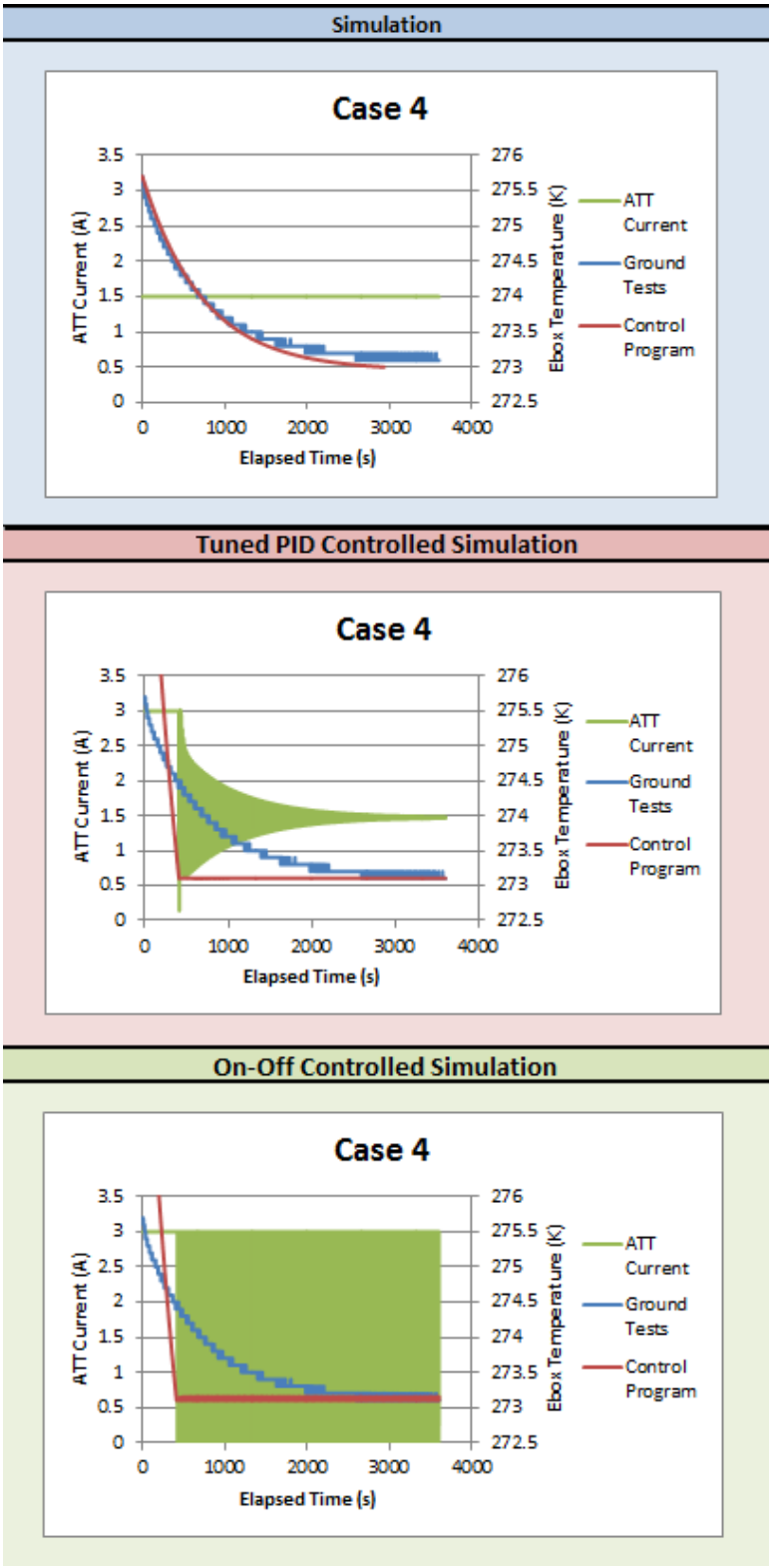

Figure 37: Comparison of ATT current and electronics box temperature versus time for the different control methods for Case 4 (-5K temperature differential created by a radiator temperature of 280K, an electronics box power of 5W, and an ATT current of 1.0A.)

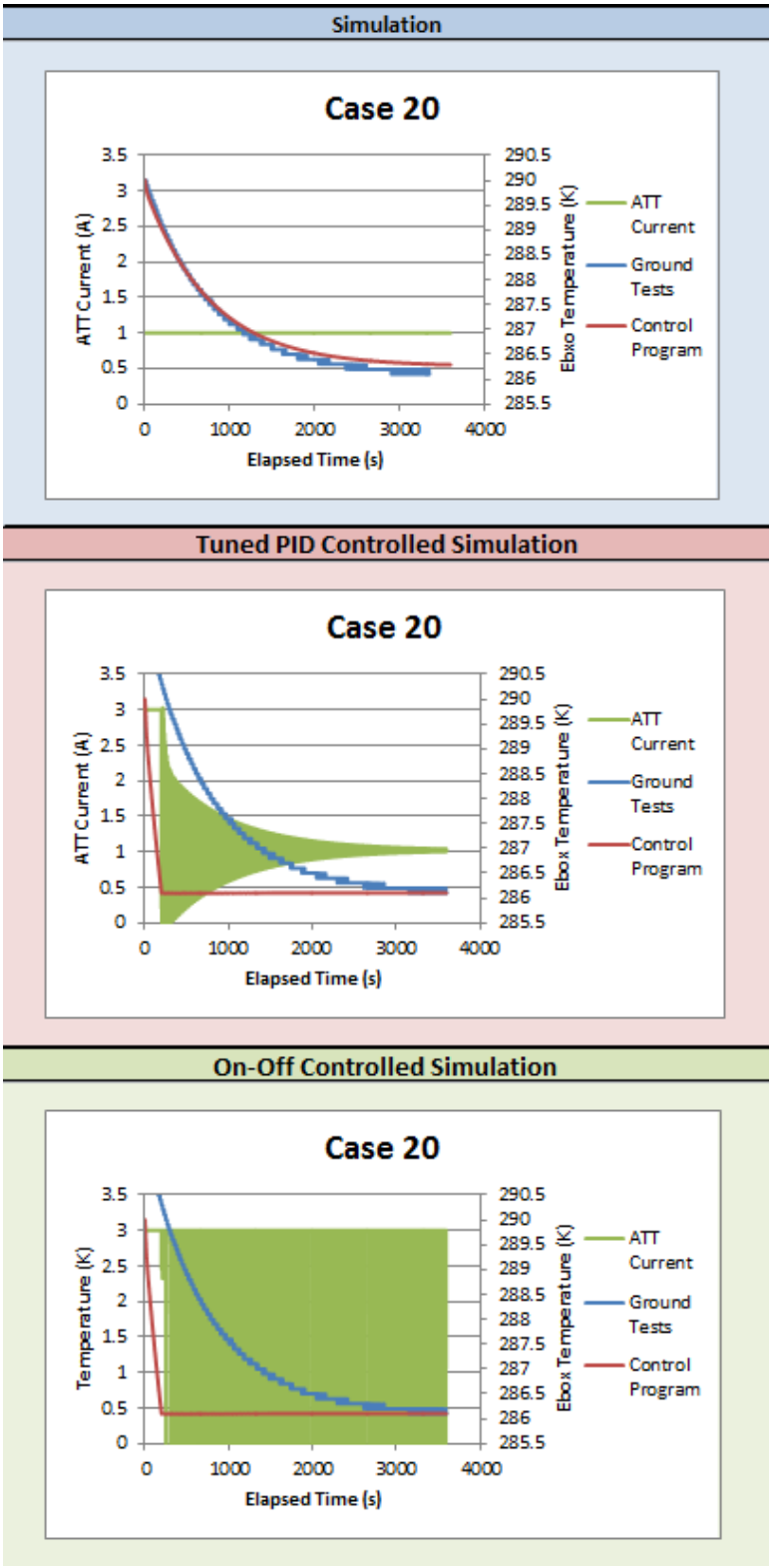

Figure 38: Comparison of ATT current and electronics box temperature versus time for the different control methods for Case 20 (-5K temperature differential created by a radiator temperature of 290K, an electronics box power of 5W, and an ATT current of 1.0A.)

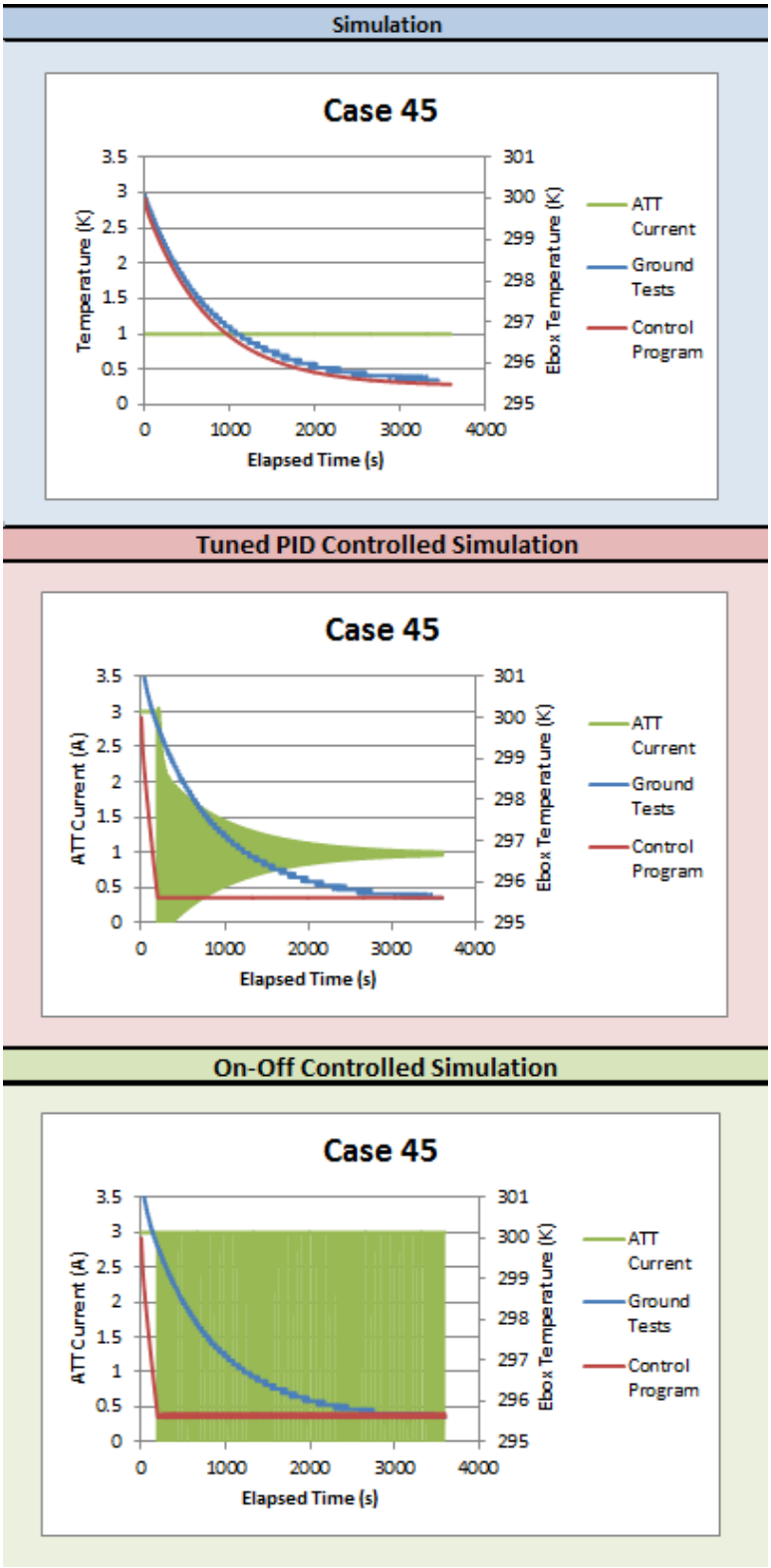

Figure 39: Comparison of ATT current and electronics box temperature versus time for the different control methods for Case 45 (-5K temperature differential created by a radiator temperature of 300K, an electronics box power of 5W, and an ATT current of 1.0A.)

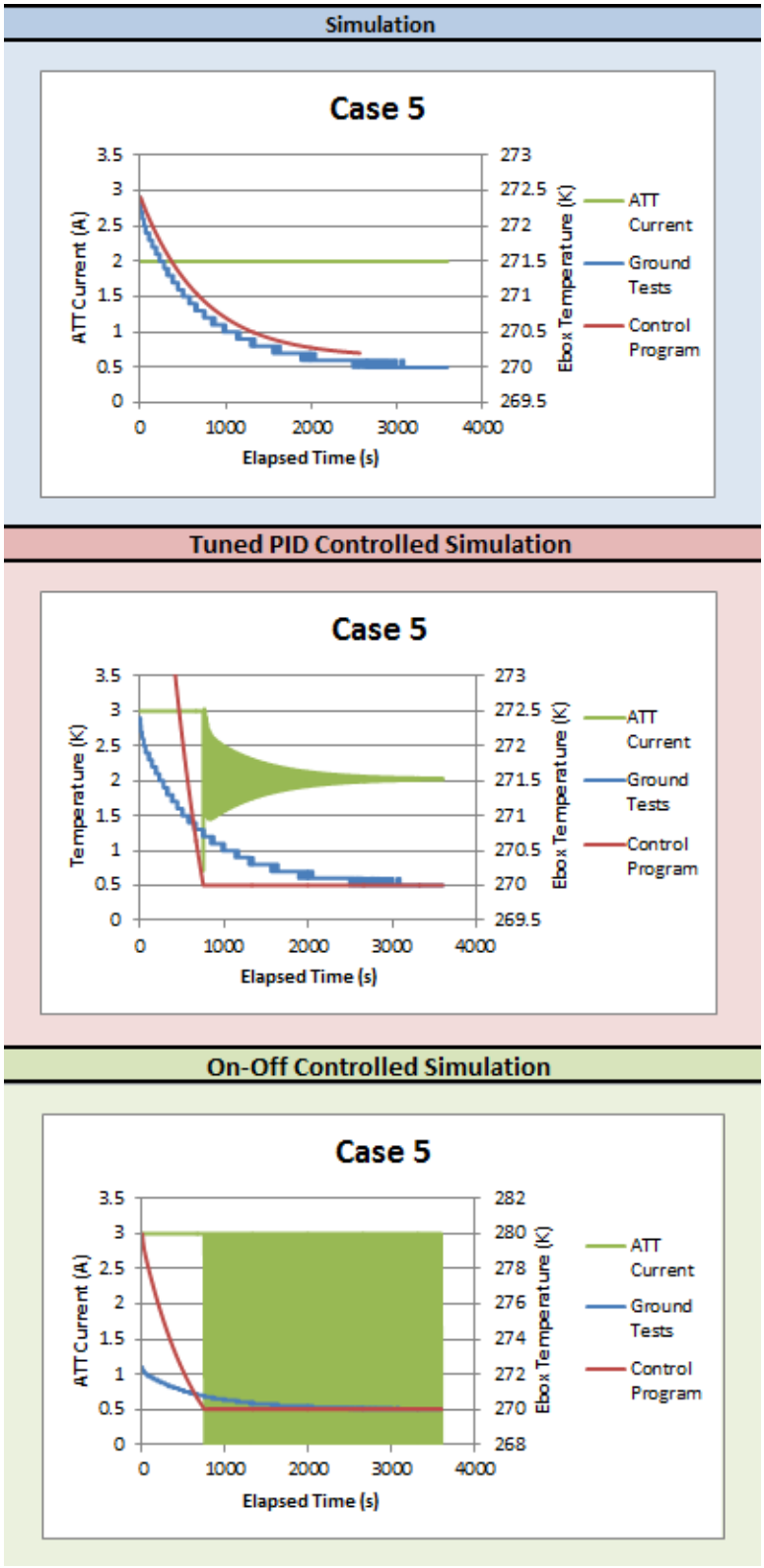

Figure 40: Comparison of ATT current and electronics box temperature versus time for the different control methods for Case 5 (-10K temperature differential created by a radiator temperature of 280K, an electronics box power of 5W, and an ATT current of 1.5A.)

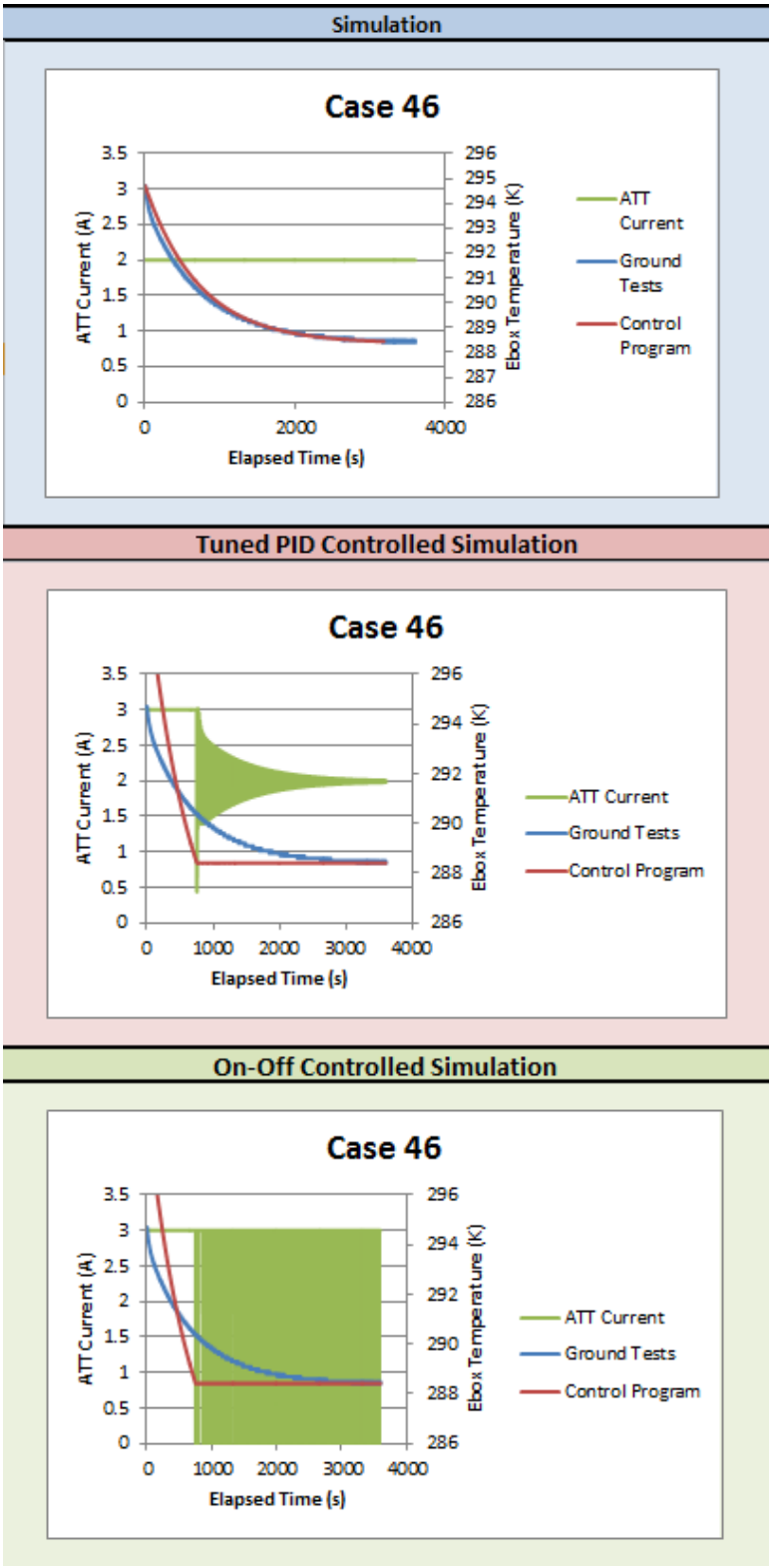

Figure 41: Comparison of ATT current and electronics box temperature versus time for the different control methods for Case 46 (-10K temperature differential created by a radiator temperature of 300K, an electronics box power of 5W, and an ATT current of 2.0A.)

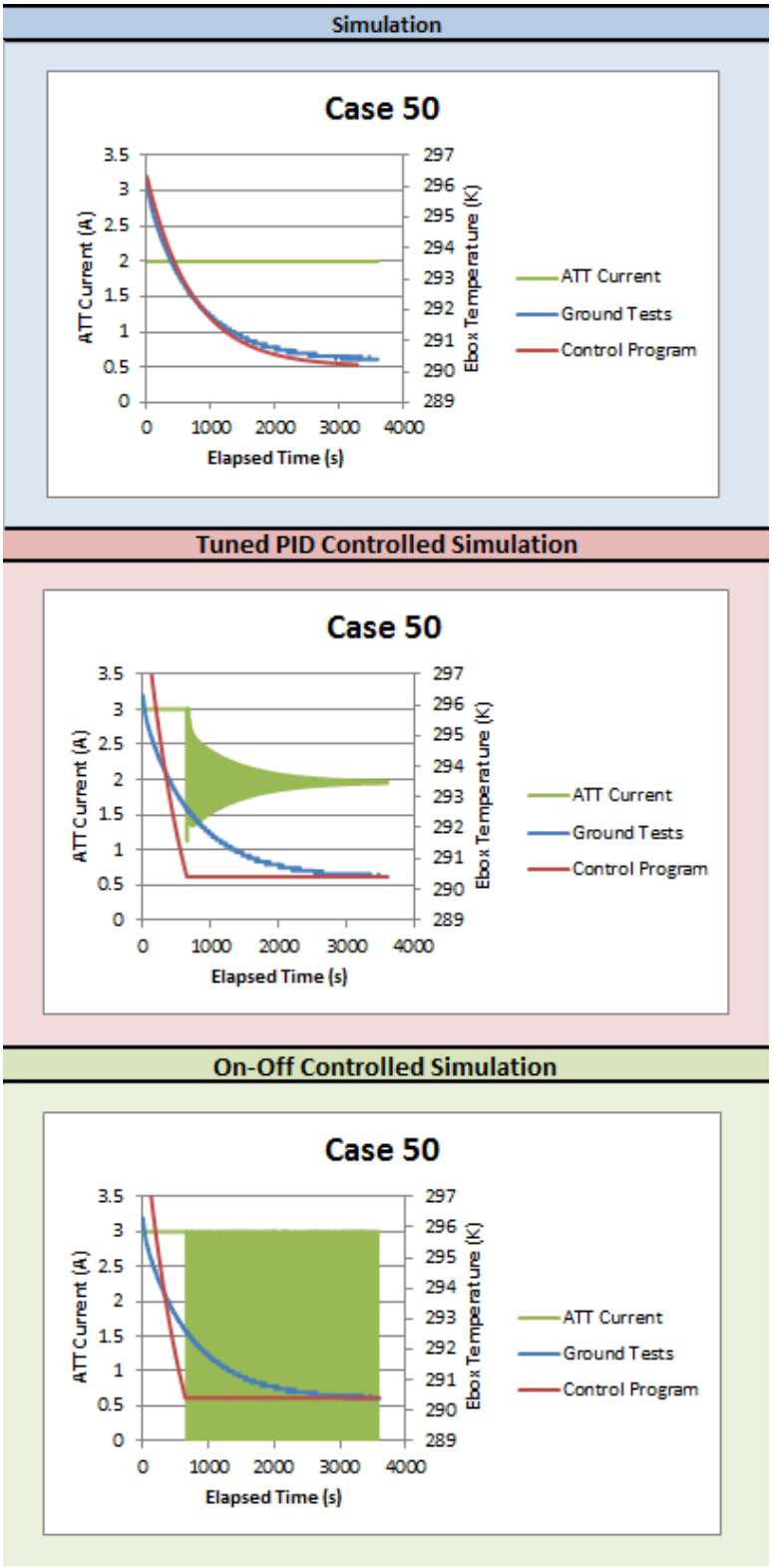

Figure 42: Comparison of ATT current and electronics box temperature versus time for the different control methods for Case 50 (-10K temperature differential created by a radiator temperature of 300K, an electronics box power of 8W, and an ATT current of 2.0A.)

Table 8: Final results for control program. Note the energy values are for TEDs only. ECU power is not included.

	Performance Test			PID			On/Off		
Case	**Avg. Temp [K]**	**Avg. Curr. [A]**	**Total Energy [J]**	**Avg. Temp. [K]**	**Avg. Curr. [A]**	**Tot. Energy [J]**	**Avg. Temp. [K]**	**Avg. Curr. [A]**	**Tot. Energy [J]**
4	273.1	1.500	9088	273.1	1.484	9323	273.2	2.847	35207
20	286.1	1.000	4049	286.1	1.035	4807	286.1	2.868	34927
45	295.6	1.000	4326	295.6	0.981	4244	295.6	2.842	35466
5	270.0	2.000	16493	270.0	2.035	17210	270.0	2.826	35545
46	288.4	2.000	18429	288.4	1.998	18531	288.4	2.846	39315
50	290.4	2.000	17860	290.4	1.967	17446	290.4	2.847	38169

The large difference between the simulated energies and the ground test energies could have several different explanations, but most likely, it is that other unknown factors are affecting the simulation results. For example, the ATTs are generating their own heat that they then have to displace. This causes them to have to remain on longer and therefore use more energy.

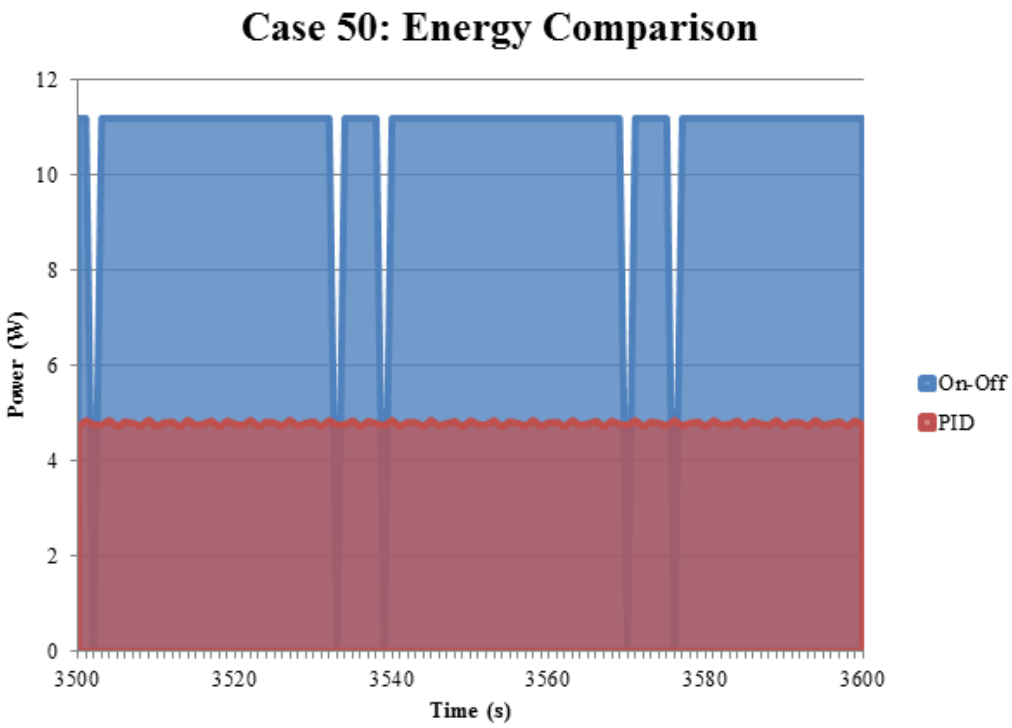

Figure 43: Energy comparison simulation example for a -10K temperature differential.

Table 9: Percent differences in energy usage over an hour between simulated On-Off control and PID control.

ΔT	Case	% Difference in Energy Usage
-5K	**4**	278%
	20	627%
	45	736%
-10K	**5**	107%
	46	112%
	50	119%

5.2. Ground Testing Results

After examining the simulations, the same cases were run on the flight spare to verify the data created by the simulator. The results of these tests are shown in Table 10. It was found that the ground tests produced similar average temperatures, ATT currents, and total energy values to the simulation for the PID cases. There was a significant

difference between the values from the ground test and the simulation for the On-Off cases. The percent differences between the simulation and the ground tests are shown in Table 11. Not only were there large differences in the values for the On-Off cases, but the waveforms for the two testing methods were shaped differently as well, as shown in Figure 44. The simulation waveforms for the PID controlled cases remained nearly constant throughout steady state. The ground test waveforms for the PID controlled cases, on the other hand, fluctuated throughout steady state.

Table 10: Final results for the ground testing.

	PID			On/Off		
Case	**Avg. Temp. [K]**	**Avg. Curr. [A]**	**Tot. Energy [J]**	**Avg. Temp. [K]**	**Avg. Curr. [A]**	**Tot. Energy [J]**
4	273.2	1.466	8882	273.2	1.593	15488
20	286.2	0.982	4187	286.1	1.091	9986
45	295.7	0.977	4343	295.6	1.058	9529
5	270.2	1.951	15870	270.1	2.090	23165
46	288.6	1.953	17939	288.5	2.040	22993
50	2906	1.957	17485	290.5	2.048	22612

Table 11: Differences between the ground tests and control simulations.

	PID			On/Off		
Case	**Avg. Temp. [K]**	**Avg. Curr. [A]**	**Tot. Energy [J]**	**Avg. Temp. [K]**	**Avg. Curr. [A]**	**Tot. Energy [J]**
4	0.05%	-1.20%	-4.73%	0.00%	-44.05%	-56.01%
20	0.02%	-5.15%	-12.90%	-0.02%	-61.96%	-71.41%
45	0.02%	-0.40%	2.33%	-0.02%	-62.75%	-73.13%
5	0.07%	-4.09%	-7.79%	0.04%	-26.04%	-34.83%
46	0.06%	-2.20%	-3.19%	0.02%	-28.33%	-41.52%
50	0.06%	-0.50%	0.22%	0.03%	-28.06%	-40.76%

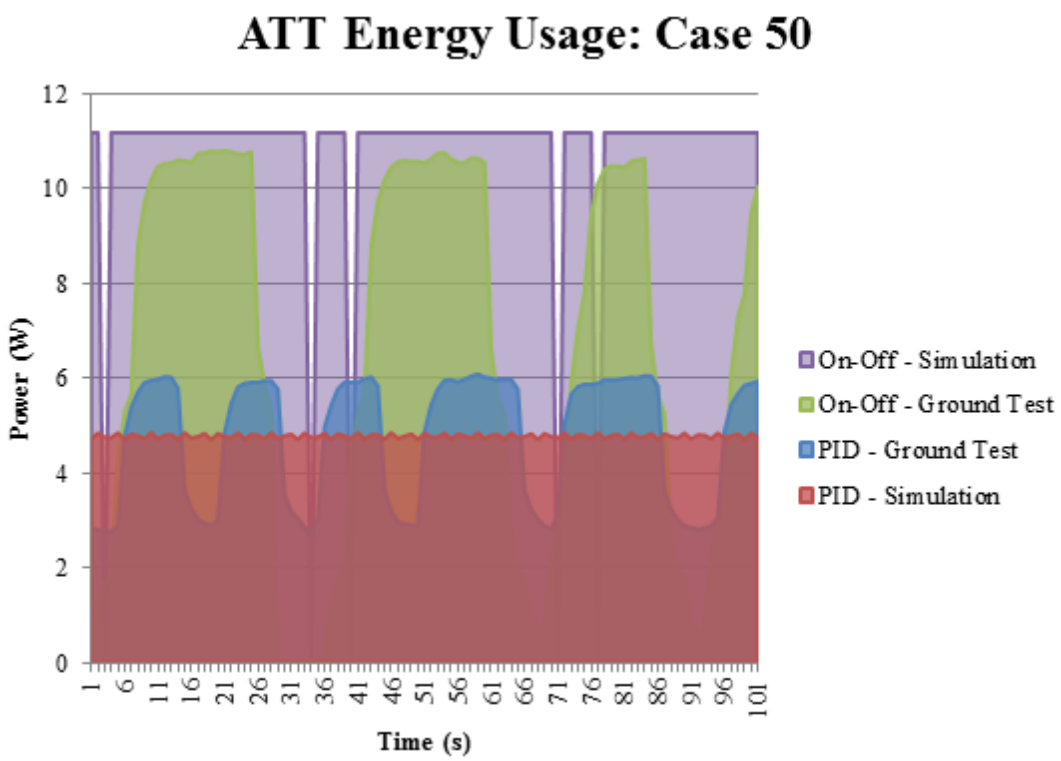

Figure 44: Energy comparison between the ground tests and the simulation for a -10K temperature differential.

While the ground tests proved that the PID control was indeed more efficient than On-Off control, the waveforms did not come out as expected. The total energy values from the ground tests were more reasonable than the energy values from the simulation, but the waveforms were not. This was a problem since the On-Off cases were supposed to result in currents of either 0.0A or 3.0A. Instead, they varied in discrete steps between 0.0A and 3.0A as shown in Figure 45.

When the experiment is current controlled, the system adjusts the voltage to allow the current to rise to the level it needs to be to reach the proper temperature. However, the program only checks the current value to adjust the voltage value every three seconds. Also, there is a limit to how high the voltage can rise instantaneously. That limit is 1.0V corresponding to 1.0A for the four TEDs in series. This means that when TED current is

supposed to jump to 3.0A, it will only do so in 1.0A increments every 3 seconds. This is not the case when the TEDs are turning off. When the TEDs are required to turn off, the current will instantaneously turn off instead of following the pattern it follows when the current rises. This explains the strange waveforms obtained for the ground tests run by the On-Off control method.

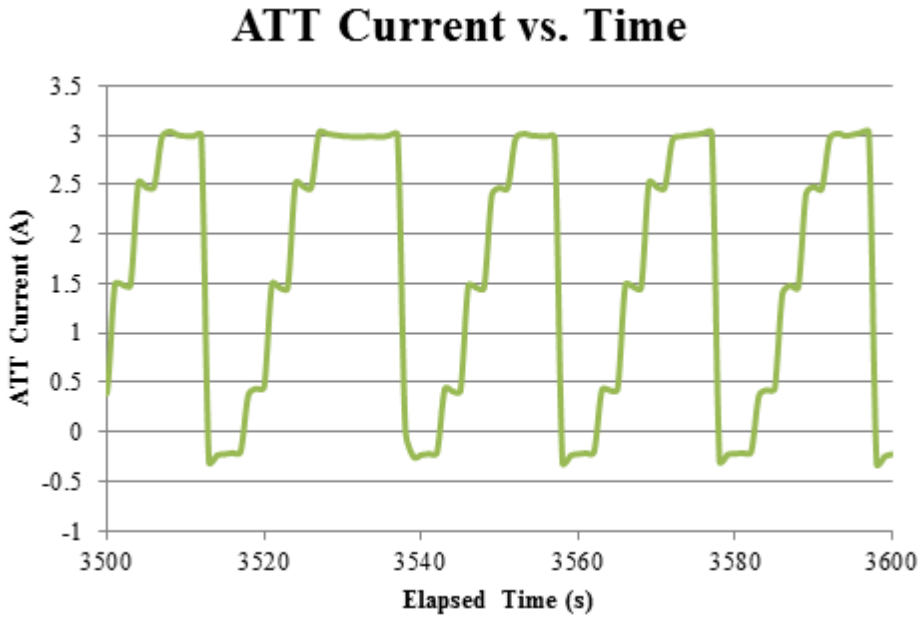

Figure 45: ATT current versus elapsed time for On-Off case ground test.

This still did not explain the strange waveform for the PID cases during the ground tests. A range of gains was tested on the ground experiment to validate the gain value the simulation gave. To do this, average steady state electronics box temperature and total energy used over an hour were graphed versus the gain values. For, most cases, as the gain increased, temperature decreased, but only by a small increment. Second, as gain increased, total energy used over an hour increased. Overall, the different gains did not produce significant changes in temperature. So the gain predicted by the simulation may not be the optimum gain, but it might not make a significant difference.

It was also noticed that there is a gain threshold that significantly impacts energy usage. Case 20, shown in Figure 46, is a good example of this. Temperature decreases an average of 0.04K with every 250A/K increase in the proportional gain; energy rises by over 200J with each gain increase. In addition, there is a large spike in the energy plot with an increase in gain from 1000 A/K to 1250 A/K; when the gain is 1250 A/K, the total energy used is more than twice the energy used when the gain was 1000 A/K. Up until a certain value between 1000 A/K and 1250 A/K for Case 20, the changes in proportional gain have little impact on temperature or energy consumed over an hour. Then, at a gain of 1250 A/K, there is a significant increase in energy usage although the temperature change is remains small. This is the point at which the gain becomes oversaturated and the control method becomes On-Off control rather than PID control.

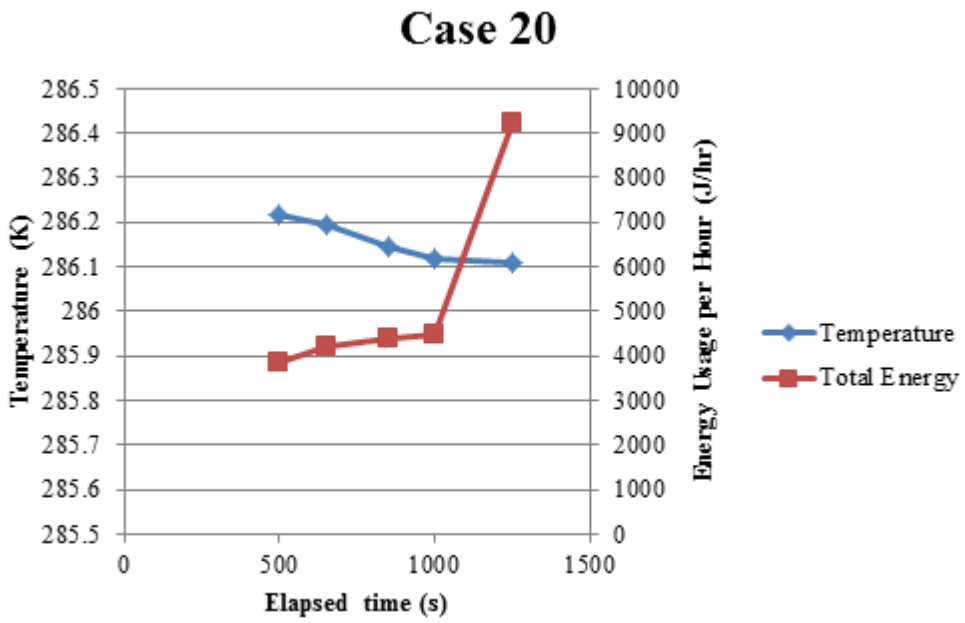

Figure 46: Electronics box temperature and energy usage per hour versus gain for Case 20.

Cases 20 and 45 both demonstrate this behavior. The rest of them did not, but comparing the energies for both the PID control and the On-Off control, the values that

can be expected after the jump would be similar to those energy values from the On-Off cases. With more time, more ground testing could be conducted, and this point were the energy usage significantly increases could be found.

5.3. Uncertainty Analysis

Standard deviation and resolution of the values given by the program were factored into finding the uncertainty of both the delivered and calculated values. These results are shown in Table 12 and Table 13, respectively, for the PID controlled and On-Off controlled simulations. The maximum uncertainty for the PID values is only ±4.00% once the ATT current has converged on a current value. However, the maximum uncertainty for the On-Off cases is much higher – over ±30%. This is because during the On-Off cases, the current fluctuates between 0A and 3A as opposed to fractions of an amp.

Table 12: Uncertainty percentages for PID controlled simulation.

Delivered		**Calculated**	
Value	**% Uncertainty**	**Value**	**% Uncertainty**
Ebox Temp	±0.00%	ATT Power	±4.00%
ATT Current	±2.53%	ATT Energy	±4.00%

Table 13: Uncertainty percentages for On-Off controlled simulation.

Delivered		**Calculated**	
Value	**% Uncertainty**	**Value**	**% Uncertainty**
Ebox Temp	±0.01%	ATT Power	±32.06%
ATT Current	±22.63%	ATT Energy	±32.06%

6. Conclusion and Future Work

Active Thermal Tiles (ATTs) were tested over a range of possible methods of operation. Of interest in this study was the ATT's cooling capability, heating capability as compared to survival heaters, and control methods efficiency.

The cooling cases verified the ATTs cooling capacity. In all, a total of 72 cases were tested and two performance maps were created: a map relating the temperature differential to ATT current, and a map relating the temperature differential to ATT power. The first map (Figure 27) showed that the performance of the ATTs depends on the temperature gradient created between the radiator and the electronics box. This graph showed that low ATT currents result in a greater positive temperature differential. High ATT currents result in a greater negative temperature differential as expected. The rate of change is about 7K for every amp, and the temperature difference ranges from 20K to -20K as ATT current increases. The second map (Figure 29) showed that as ATT power increases, the temperature differential will also but only to a point. At some point, joule heating will cause the ATTs to become less efficient.

The heating cases were run to compare the energy ATTs used to heat compared with that of survival heaters. Like survival heaters, they are small, lightweight, and have no moving parts. However, these tests have shown that the ATTs are more efficient in heating than the survival heaters. While both heating options require more power to create larger temperature differentials, the heaters require much more of a power increase to create the same temperature differentials as the ATTs. Other ATT advantages over survival heaters include their versatility as due to connections that allow for modular reconfiguration and their cooling capability.

Then the different control methods were evaluated. There are two modes of control: control by tuned PID constants which will find the best current to constantly run the ATTs at, or control by switching the ATTs on at full power and then off. Six cases were run via a control program which sped up the testing process, allowed different gain values to be tested, and determined the optimal gain – that is, the gain that results in the electronics box temperature matching the set point while using the least amount of energy. However, running a variety of cases with varying gains using the actual test setup, it was found that there might not be an optimal gain. Instead, there may be a gain beyond which the energy consumption doubles. There is some experimental evidence of this behavior, but it was not demonstrated for all of the test cases. As for which control method is more efficient, tests have proved that the PID control is at least twice as efficient as On-Off control.

In the future, there should be a more in-depth investigation into the control scheme for the ATTs – one that finds not only the proportional gain, but also the integral and derivative factors in a proportional-integral-derivative (PID) controller that allow the ATTs to keep the electronics box within a desired range while using the least amount of energy.

Other future tests of interest would include discovering the impact that increasing the number of ATTs would have on several aspects of ATT performance. These cases would look at the effect the number of ATTs had on COP and power usage. They would also be geared for finding the point at which the power used to cool or heat a payload would outweigh the benefits adding more ATTs would give.

Before testing can be expanded some aspects of the control setup should be changed. A board with separate grounds for the two buses which power the experimental setup should be manufactured. This would simplify the procedure by removing the post-test step. Secondly, the refrigerating bath setup should also be re-evaluated. There were several problems with cooling the radiator that stemmed from the refrigerating baths. During the summer months, humidity would cause ice to form not only in the reservoirs of the refrigerating baths, but also on the cooling apparatuses inside. This would lower the efficiency and interfere with the performance tests. Upgrades should include ways to isolate the cooled Syltherm and cooling apparatuses from the environment to allow for more efficient testing.

The data collected from these tests has been and will continue to support on-orbit operations. Overall, ATTs seem to be a promising component in temperature control of a spacecraft. ATTs have many advantages over other methods of thermal control. They offer heating and cooling capacity, and they have versatility as plug and play connections. They lack moving parts or heavy fluids and are extremely efficient when compared to survival heaters. For these reasons, ATTs are promising candidates for use on spacecraft.

References

Alley, R., Soto, M., Kwark, L., Crocco, P., and Koester, D., "Modeling and Validation of On-Die Cooling of Dual-Core CPU using Embedded Thermoelectric Devices," *Semiconductor Thermal Measurement and Management Symposium,* IEEE, San Jose, CA, 2008, pp. 77-82.

Chein, R. and Huang, G., "Thermoelectric Cooler Application in Electronic Cooling," *Applied Thermal Engineering*, vol. 24, 2000, pp. 2207-2217.

Cheng, J., Liu, C., Chao, Y., and Tain, R., "Cooling Performance of Silicon-based Thermoelectric Device on High Power LED," *24th International Conference on Thermoelectrics,* IEEE, 2005, pp. 53-56.

Coalition for Space Exploration, "Why Space Matters," 2010, [http://spacecoalition.com/benefits-of-space. Accessed 9/12/13].

Copeland, R. and Oren, J., "Cooling Systems For Satellite Remote Sensing Instrumentation," Vought Systems/LTV Aerospace Corperation, Dallas, NASA CR-132517, 1975.

DiSalvo, F. J., "Thermoelectric Cooling and Power Generation," *Science,* Vol. 285, no. 5428, 1999, pp. 703-706.

Gilmore, D., *Spacecraft Thermal Control Handbook Volume 1: Fundamental Technologies*, The Aerospace Corporation, 2002, pp. 523-534.

Hengeveld, D., "ATT Operation", Kirtland Air Force Base, NM. 2011, 1 pp.

Laird Technologies, Thermoelectric Handbook, 2010, p. 3. [http://www.lairdtech.com/Products/Thermal-Management-Solutions/Thermoelectric-Modules/. Accessed 1/11/13].

Marlow Industries, Inc., "How Efficient is a Thermoelectric Cooler?," Marlow Industries, Inc., 2012. [http://www.marlow.com/resources/general-faq/14-how-efficient-is-a-thermoelectric-cooler.html. Accessed 1/10/13].

Marlow Industries, Inc., "Technical Data Sheet: XLT2391 Single-Stage Thermoelectric Cooler," Marlow Industries, Inc., Doc # 102-0236, 2012.

Mole, C. J., Foster, D. V., and Feranchak, R. A., "Thermoelectric Cooling Technology," *IEEE Transactions on Applications and Industry,* Vols. 1A-8, no. 2, 1972, pp. 108-126.

National Aeronautics and Space Administration, "Spacesuits and Spacewalks: Fact Sheet," 2012, [http://www.nasa.gov/audience/foreducators/spacesuits/facts/facts-index.html. Accessed: 1/8/13].

Nolas, G., Slack, G., Cohn, J., and Schujman, S., "Next Generation of Thermoelectric Materials," *International Conference on Thermoelectrics*, IEEE, 1998, pp. 294-297.

Peabody, H., Stavley, R., and Bast, W., "Lessons Learned from the Wide Field Camera 3 TV1 Test Campaign and Correlation Effort," in *Thermal Fluids Analysis Workshop Proceedings*, NASA, 2007.

Ramanathan, S. and Chrysler, G., "Solid-State Refrigeration for Cooling Microprocessors," *IEEE Transactions on Components and Packaging Technologies,* vol. 29, 2006, pp. 179-183.

Riffat, S. B. and Ma, X., "Thermoelectrics: A Review of Present and Potential Applications," *Applied Thermal Engineering,* vol. 23, no. 8, pp. 913-935, 2003.

Simons, R. E. and Chu, R. C., "Application of Thermoelectric Cooling to Electronic Equipment: A Review and Analysis," *Sixteenth Annual IEEE Semiconductor Thermal Measurement and Management Symposium*, 2000, pp. 1-9.

Tiezhu, Z., Yaqing, Q., Jianzhong, Z., Qinghua, W., Yonglong, Y., Fang, L., and Liang, H., "Thermoelectric Cooler for Space Microgravity Experiment," *Eighteenth International Conference on Thermoelectrics*, IEEE, 1999, pp. 325-327.

Walker, D. G., Frampton, K. D., and Harvey, R. D., "Distributed Control of Thermoelectric Coolers," *The Ninth Intersociety Conference on Thermal and Thermomechanical Phenomena in Electronic Systems*, vol. 1, IEEE, 2004, pp. 361-366.

Wang, P., Bar-Cohen, A. and Yang, B., "Enhanced Thermoelectric Cooler for On-Chip Hot Spot Cooling," *Proceedings of the ASME InterPACK Conference,* 2007, pp. 249-258.

space-exploration.org, "Benefits of Space Exploration", 2013, [http://www.space-exploration.org/?page_id=12. Accessed 9/12/13.]

Wijngaards, D., Kong, S., Bartek, M. and Wolffenbuttel, R., "Design and Fabrication of On-Chip Integrated PolySiGe and PolySi Peltier Devices," *Sensors and Actuators: A Physical,* vol. 85, no. 1-3, 2000, pp. 316-325.

Williams, A. and Hengeveld, D., *Active Thermal Tile (ATT): Test Plan for Flight Operations,* Kirtland Air Force Base, 2011

Yeh, L. and Chu, R., Thermal Management of Microelectronic Equipment: Heat Transfer Theory, Analysis Methods, and Design Practices, ASME Press, New York, 2002, pp. 335-337.